C.P. No. 946

C.P. No. 946

MINISTRY OF TECHNOLOGY

AERONAUTICAL RESEARCH COUNCIL

CURRENT PAPERS

An Analogue Computer for On-Line Correction of Wind-Tunnel Force and Moment Data

by

B. E. Pecover

LONDON: HER MAJESTY'S STATIONERY OFFICE

1967

PRICE 9*s* 6*d* NET

U.D.C. No.681.14 : 621.317.79 : 533.6.071 : 533.6.011.5 : 533.6.013.11 : 533.6.013.15 : 531.71

*C.P. No.946

October 1966

AN ANALOGUE COMPUTER FOR ON-LINE CORRECTION OF WIND TUNNEL FORCE AND MOMENT DATA

by

B. E. Pecover

SUMMARY

A description is given of equipment using analogue computing techniques for the on-line correction of wind-tunnel force and moment data, derived from strain-gauge indicator servos operating with a supersonic wind tunnel.

This equipment has enabled a new method of balance calibration to be employed which considerably reduces the possibilities of error and is quicker than previous methods.

Accuracy is discussed and comparisons made between results obtained from the new equipment and those obtained by earlier, digital techniques.

*Replaces R.A.E. Technical Report No.66318 - A.R.C. 28,858

CONTENTS

1 INTRODUCTION

Force and moment measurements on models in the high speed wind tunnels at R.A.E. are made by the use of strain gauge balances. Usually components along and about a right-angled axis system fixed in the model are measured. The measurements are recorded on servo indicators, which are developed versions of those described in Ref.1, so that a change in a particular component results in a change of shaft position in its associated indicator.

Although an individual section of the balance is designed to measure an individual component, it usually has some sensitivity to other components. The data obtained from the balance then require correction to eliminate the interactions thus arising. Other corrections are necessary for changes in model tare components with attitude, variations in kinetic pressure, erroneous base pressures, temperature drifts in the strain gauges.

The practice has been to equip the servo indicator shafts with digitisers, thus enabling the uncorrected data to be recorded on punched cards or tape. These data were subsequently used together with the balance calibration data to obtain the corrected results via a digital computer. Thus the results of a test would not be available until several days after its completion. This delay is undesirable for several reasons; for instance a need for further data points may become apparent only upon inspection of the corrected data, so that the expense of re-running a test is incurred which could have been avoided had corrected results been immediately available.

However desirable on-line data correction may be for conventional tests, for the flight dynamics simulator[2] installation using the R.A.E. No.19 wind-tunnel it is essential. In this application a new set of corrected data must be available within two milliseconds of the model attitude changing.

This report describes the tare correction unit and analogue correction unit now used by the No.19 wind-tunnel system to meet data correction needs both for the simulator and conventional tests. The former was specially built to work with the particular type of servo indicator in use whereas the latter is not so restricted in its application.

Before deciding to employ analogue computing techniques for data correction, consideration was given to digital and D.D.A. techniques but it was found that analogue equipment could meet the speed and accuracy requirements at least cost.

This report includes a comparison of results obtained using the analogue correction unit with those from the same raw data processed by digital computer.

The tare correction unit was manufactured within R.A.E. The analogue correction unit was designed and manufactured by Messrs. Redifon Ltd., Crawley, Sussex to R.A.E. Specification Number TFEQ 357-2.

2 THE TARE CORRECTION UNIT

If the balance has channels nominally measuring components of force (X, Y, Z) along and moment (L, M, N) about a right angled axis system Ox, y, z, fixed in the model, of weight w and the centre of gravity of which is x_g along the Ox axis, then the tare components listed in Table 1 will also be measured. In this table σ denotes the incidence and λ the roll angle, ε_x, etc. are misalignments due to the same balance imperfections which cause interactions.

Table 1

Tare components

Channel	Tare component	Approximation
X	$w \sin(\sigma + \varepsilon_x)$	-
Y	$w \cos\sigma \sin(\lambda + \varepsilon_y)$	$w \sin(\lambda + \varepsilon_y) - w \frac{\sigma^2}{2} \sin\lambda$
Z	$w \cos\sigma \cos(\lambda + \varepsilon_z)$	$w \cos(\lambda + \varepsilon_z) - w \frac{\sigma^2}{2} \cos\lambda$
L	Nil if C.G. lies on	Ox axis
M	$wx_g \cos\sigma \cos(\lambda + \varepsilon_m)$	$wx_g \cos(\lambda + \varepsilon_m) - wx_g \frac{\sigma^2}{2} \cos\lambda$
N	$wx_g \cos\sigma \sin(\lambda + \varepsilon_n)$	$wx_g \sin(\lambda + \varepsilon_n) - wx_g \frac{\sigma^2}{2} \sin\lambda$

To simplify the computing the approximation shown in the table has been adopted. This involves an error rising roughly as the fourth power of incidence to a value of 0.15% of the tare contribution at the maximum incidence obtainable (25°). Since the tare contribution is likely to be considerably smaller than the aerodynamic contribution to the balance output at this incidence the error due to the approximation as a percentage of balance output is not significant. Since in some circumstances (particularly models restricted to small incidences) the changes in tare components can be quite large compared with the aerodynamic

forces being measured, it was decided to apply compensation for the first term of the approximation within the servo indicators themselves in order to keep the excursions due to tare loads small and the useful range of the instruments a maximum. The principle adopted is to develop signals equal and opposite to the balance outputs due to tare component changes, and to sum those signals with the appropriate balance outputs at the servo amplifier inputs. To this end the tare correction unit is provided with two shafts driven by servo systems to follow the tunnel incidence and roll angles respectively. The shafts are equipped with sine/cosine potentiometers supplied via padding resistors from the balance power supply. The outputs of the potentiometers are passed through variable "sensitivity" resistors for scaling the size of the correction (w or wx_g) and thence to the servo amplifier input. The alignments of the potentiometers are individually adjustable over a range of about 40° to enable their outputs to be exactly anti-phased with the balance outputs. Fig.2, shows diagrammatically the arrangement for one channel.

A nulling procedure is adopted for setting up the correction and is most easily performed with the aid of an X-Y plotter. The most sensitive range of the servo indicator is always used during setting up since the setting holds good for all sensitivities but is most accurately found using this range. A plot is made of indicator reading versus some convenient function of the attitude parameter causing the change in tare component, for instance K sin λ, and adjustments are made to the phase of the sin/cos potentiometer and the "sensitivity" controls of the particular channel of the tare correction unit until a horizontal straight line is achieved within the desired accuracy. A typical example of the result of this procedure is shown in Fig.3, where it can be seen that correction is possible to within ±0.2% of full scale on the maximum indicator sensitivity. Also plotted in this figure is the highly satisfactory result of this compensation at the indicator sensitivity used in practice for this particular balance component.

Dynamic performance is indicated in Fig.4, where various rates of roll are used and little increase in error is apparent in this range of roll rates.

Analogues of $\sigma^2 \sin \lambda$ and $\sigma^2 \cos \lambda$ are generated by means of linear and sin/cos potentiometers as indicated in Fig.5. These analogue voltages are fed into the analogue correction unit at appropriate parts of the system as indicated in Fig.7. Since these provide very small corrections there is no fine phase adjustment. The sensitivity controls for setting w and $\pm wx_g$, are on the analogue correction unit programme panel, see Fig.6, and Fig.7, potentiometers g_2, g_3, g_5 and g_6.

The setting-up procedure in this case is merely a matter of setting values on the 'g' potentiometers which make the analogue correction unit outputs at large incidence the same as those at zero incidence, at appropriate roll angles.

3 ANALOGUE CORRECTION UNIT PROGRAMME

3.1 Production of voltage analogues of raw data

Voltages proportional to raw data readings are produced by potentiometers fitted to the output shafts of the servo indicators or gear driven by the Midwood manometers[3] which are used to measure base pressure P_{b_1} and P_{b_2} and stagnation pressure H_T.

The potentiometers used are compatible with the accuracies of the instruments concerned - 0.1% law accuracy for the servo indicators and 0.025% for the manometers, although the latter does represent a very slight degradation. The potentiometers are supplied from one or other of the correction unit reference supplies which are plus or minus 100 volts, stable to within ±0.02 volts.

Thus 100 volts represents the full scale reading of 100% of indicator shaft rotation or 120 or 60 inches of mercury absolute pressure, depending on the manometers in use.

3.2 Datum shift

The servo indicator can be set to any shaft position for no input, and changes in input can then be measured from that position as datum. This leads to the need for calculations of the form $R = E - E_o$, where R is the change in position due to an input which gives a position E, the datum position having been E_o.

To facilitate this, "zero set" potentiometers are provided, fed from the negative reference supply, whose outputs are summed with the (positive) outputs of the servo indicator driven potentiometers.

3.3 Temperature correction

Strain gauge balances are usually somewhat temperature sensitive, although those with a marked sensitivity are rejected. The stagnation temperature in the No.19 tunnel can be controlled within ±1°C and it is usual to arrange it so that the balance remains close to room temperature during tests, thus minimising drifts. Small drifts in balance output nevertheless sometimes occur which can often be linearly related to a temperature measured somewhere on the balance. The practice is to place thermistors at up to three strategic places on the balance so that the most appropriate temperature reading can be related to each component output by calibration.

We then obtain six equations for notional changes in indicator readings, due to changes in force or moment only, of the following form:

$$R_F = E_F - E_{F_o} + K_F(\pm R_{TA}) .$$

Where suffix F refers to force or moment channels X, Y, Z, L, M or N, K is a calibration factor and R_{TA} is defined by

$$R_{TA} = E_{TA} - E_{TAO} .$$

Where suffix T refers to a temperature channel specified by A = 1, 2 or 3.

In the correction unit any of the three voltage analogues of R_{TA} can be selected to provide a correction of the required sign for any force or moment channel. The selector switches shown in Fig.7 determine which voltages are fed to the temperature correction scaling potentiometers K_F.

3.4 Corrections for interactions

In a well designed strain gauge balance interactions, by which is meant sensitivity to components of force or moment other than the desired one, are fairly small and linear to the accuracy of the indicator. An exception has been the axial force component in some balance designs, in which sensitivity to cross products or squares of various components has been present. In particular, calibrations of the axial components of balances in which the axial force unit is at the rear contain such terms, which arise from the misalignment of axial component and model axes caused by sting bending under normal or side loads. In the latest designs[4] these terms are minimised by geometry giving high stiffness and compactness.

Provided there are no interactions of axial force on the other components then correction for cross product sensitivity in this channel may be accomplished conveniently. The digital data reduction programme currently in use accepts such terms together with the above restriction and it is possible to devise ways of so doing using analogue techniques (see for instance the layout in Fig.2 of Ref.2). However, a case can now be made that it is more generally useful to correct for all possible linear interactions and to exclude cross product sensitivity terms (not precluding their correction in some off-line processing if necessary in special cases). This course certainly requires less equipment and is adopted for the correction unit described here.

In order to eliminate interactions it is necessary to find a, b, etc. in the matrix composed of six equations, each of form

$$F = a_F R_X + b_F R_Y + c_F R_Z + d_F R_L + e_F R_M + f_F R_N$$

where F is X, Y, Z, L, M, N successively.

In the digital correction procedure the corresponding coefficients in the inverse matrix are first found by the method described in Ref.5 and this matrix is then inverted to obtain the required form above.

In the analogue correction unit, to save equipment and maintain accuracy, the coefficients of R_F are normalised with respect to the leading coefficient in each equation and six J_F F are generated. J_F is the reciprocal of each leading coefficient before normalisation and is automatically cancelled in the final scaling procedure. The normalised coefficients are then effectively set up by potentiometers supplied with either positive or negative voltage analogues of R_F according to the sign of the coefficient in question. The setting up procedure consists in using the potentiometers to null the interactions apparent when the leading terms only are present, as described in section 4.2.

Also added at this stage are the second order tare correction terms, and provision is made for including in the summation externally generated voltages, Sc, which could for instance be used to represent thrust.

Inputs to the summing amplifiers computing J_F F are via patch leads so as to provide maximum flexibility in programming.

3.5 Base pressure correction

Due to sting interference the base pressures, P_b, acting on the model are usually non-representative of flight conditions. It is then the custom to apply corrections to the measured axial force as that the result corresponds to a condition in which there is free stream static pressure on the base. In common with the current digital correction programme, corrections for up to two different base areas exposed to different unrepresentative pressures are permitted. Since at constant Mach number free stream static pressure bears a constant relation to stagnation pressure, H_T, the following calculation of corrected axial force is made.

$$J_X X' = J_X X + K_1 H_T + K_2(-P_{b_1}) + K_3(-P_{b_2})$$

where K_1, K_2 and K_3 are constants set by potentiometers whose inputs are voltage analogues of H_T, P_{b_1} and P_{b_2}.

3.6 C.G. shift facility

There is sometimes a need to compute pitching and yawing moments about reference points (i.e. C.G. positions) other than those implied in the balance calibration matrix.

In the case of pitching moment, for instance, this involves generating $J_M M'$ where

$$J_M M' = J_M M + x_1 J_Z Z \quad ,$$

x_1 being the distance moved.

To facilitate the solution this is rewritten

$$J_M M' = J_M M + x_1(\pm J_Z Z)$$

x_1 now always being positive and the sign of $J_Z Z$ chosen appropriate to the direction of C.G. shift. If a potentiometer is used to set x_1 the maximum shift is limited by $x_1 \not> 1$. To overcome this restriction provision is made for generation of the alternative form

$$J_{M'} M' = \pm J_Z Z + \frac{1}{x_1} J_M M$$

where $J_{M'} = J_M/x_1$.

A patchboard is provided to allow either form of the equation to be used; the potentiometer sets either x_1 or $1/x_1$ as appropriate.

Similar arrangements are provided for yawing moment shift x_2. Although normally x_1 and x_2 would be the same, the correction unit does not make this obligatory.

3.7 Sting bending correction

If the model attitude is to be known accurately it is necessary to compute the deflection of the balance under load. Deflections about the roll axis are normally small enough to be ignored, and the other components of deflection, $\Delta\alpha$ and $\Delta\beta$, are computed from the following equations:-

$$-\Delta\alpha = A_1 J_Z Z + B_1(-J_M M)$$

$$-\Delta\beta = A_2 J_Y Y + B_2 J_N N \quad .$$

The coefficients A_1 etc. are set on potentiometers, the appropriate values being determined during balance calibration.

3.8 Normalisation with respect to kinetic pressure

In conventional tests the output data are required as coefficients, $C_F = F/qS$, where q is the stream kinetic pressure and S is a reference area or volume of the model as appropriate, but for simulation purposes forces and moments appropriate to full scale must be generated.

Since the tunnel kinetic pressure is not necessarily constant nor that at full scale, the approach adopted in the analogue correction unit is to generate the quantity F/q, where q is the tunnel kinetic pressure, and to provide for individual scaling of each output channel. This allows coefficients to be obtained if required by arranging that the scale factor represents 1/S or alternatively permits generation of full scale forces and moments appropriate to any constant altitude in which case the scale factor represents the full scale kinematic pressure. Compensation for variations of altitude is conveniently achieved in the associated computers (Corsair D.D.A's) when necessary to the simulation.

The requirements are met by solving the equation $F/q = J_F F V_S G_F/H_T$ for each of the six components using a servo divider. G_F are adjustable gains of the output amplifiers, V_S, the servo divider standard voltage, is also a preset scaling factor common to all outputs when the test Mach number is constant, since q/h_T is then constant. One reason for using this form of division is that if a variable Mach number nozzle is eventually provided for the tunnel it will still be possible to generate coefficients, or outputs suitable for the simulator, by coupling the Mach number selecting control so as to vary V_S in an appropriate manner, otherwise retaining the same arrangement.

The final scaling (G_F) is by variable gain amplifiers rather than by potentiometers so as to obtain the low output impedance required by the simulator equipment.

The variation in output provided is such that with $H_T = V_S$ and servo indicator datum positions in mid-scale, the output for full swing of servo indicator shaft position can be set anywhere in the range ±22V to ±2V.

Fig.6 shows the layout of the programme panel and Fig.7 shows the schematic layout of the analogue correction unit.

4 CALIBRATION TECHNIQUE

To facilitate programming the correction unit, it incorporates a digital voltmeter which can be switched to display the output of any amplifier.

It is then quite feasible to calibrate a strain gauge balance by conventional methods such as those suggested by Anderson[5] and to set up the constants so found on the machine. However, a much simpler technique can be adopted which has the merit of ensuring that no mistakes of sign or order of magnitude of constants can arise. The technique, which is a nulling procedure, is described in the following sections.

4.1 Temperature calibration

While the balance is slowly temperature cycled, each R_{TA} is used in turn to restore each R_F to zero output and the potentiometer setting K_F required is noted. The procedure is repeated at many points in the cycle. The appropriate R_{TA} for each channel is then that which gives least spread of potentiometer settings and the correct setting is the mean of this least spread.

4.2 Cancellation of interactions

The model is mounted in the tunnel, as for test, except that the calibration equipment is fitted to it. The attitude control system[6] is used to set the model level.

The analogue correction unit scaling is set to give maximum output.

The leading terms in the six-by-six balance matrix are patched in, i.e. R_X to input 6 or 7 of the X group, see Fig.7, R_Y to input 6 or 7 of the Y group etc. The signs of R_F used are selected to give the correct sign of output as each component of force or moment is applied in turn to the model.

The maximum load along the Z model axis is then applied at the moment reference point. Sting deflection is compensated by adjustment of potentiometer A1 of the $\Delta\alpha$ computation until the model is level, since the $\Delta\alpha$ output is connected into the attitude control system.

The outputs of F/q other than Z/q are restored to zero by connecting the appropriate signs of R_Z volts to the respective J_F F summing amplifiers via potentiometer inputs and suitably adjusting the potentiometers. The potentiometer settings and the value of Z/q are noted.

The load is then moved to the furthest forward permissible position and the $\Delta\alpha$ correction adjusted by potentiometer B1 to restore the model to a level attitude. The outputs F/q, with the exception of Z/q and M/q are once more nulled using appropriate signs of R_M volts and further potentiometer inputs to the J_F F summers. Z/q is restored to the value it had when the load was at the reference point and M/q is noted, together with the potentiometer settings. The load is then moved aft of the reference point by the same amount and the outputs nulled by adjustment of the potentiometers supplied from R_m as at the forward point. The potentiometers are then set to the means of the values obtained at fore and aft loadings. The potentiometer feeding R_Z into J_MM is set to give numerically similar M/q at fore and aft loadings.

Similar procedures are carried out varying each of the other force and moment components in turn and setting the $\Delta\beta$ correction when dealing with Y and N (for which the model rolls through 90°).

If normal and/or side loads in both senses are to be experienced then calibration loads are applied in both senses in turn, and the potentiometers are set to the means of the settings obtained with loadings of each sense. Normally the differences in settings are small and if in any particular case this proves not to be so it is indicative of balance sensitivity to cross product terms. Of course correction for these is outside the scope of the equipment in the form described here, but this procedure even then results in the best compromise settings.

The whole loading and nulling programme is then repeated, since the process is inherently an iterative one, as many times as are necessary to obtain cancellation of interactions to within ±0.1% of full scale output. Certain non-linearities in balance outputs may, if present, prevent cancellation to this accuracy, others may be looked for by applying combinations of loads and examining the outputs.

The convergence of the cancellation process depends on the size of the interactions but in practical cases satisfactory cancellation may be achieved in three or four loading cycles, some of which may not need to be complete.

The method eliminates the need for matrix inversion and the possibility of misinterpretation of calibration data.

4.3 Final scaling

Normalisation with respect to stagnation pressure, H_T, is performed by a servo-divider whose standard voltage, V_S, is a factor in the final scaling. V_S must always be less than the analogue of H_T but optimum accuracy of the divider occurs when V_S is close to H_T. Now the range of H_T used with any particular set of servo indicator sensitivities (and hence any calibration) is in any case small. The highest divider accuracy is thus easily preserved and the following procedure for setting-up the scaling may be adopted.

The manometer reading H_T is made to give a value representative of that to be used in the test. V_S is set some five to ten percent less than this (sufficient to allow for the lowest test H_T to be encountered). The values of the desired outputs corresponding to maximum calibration loads are calculated for this H_T and the gains of each of the final amplifiers adjusted in turn to obtain these outputs when the loads are applied.

4.4 Base pressure correction

If the base pressure and total head are equal, e.g. "wind off", then the axial force coefficient should appear as

$$C_X = \frac{S_b}{q/H_T\, S} ,$$

where S_b is the base area, q/H_T is a constant for a given Mach number. The correction is then simply set by adjusting the settings of K_2 and/or K_3 potentiometers respectively so as to obtain the analogues of the increments in C_X calculated as above. C_X now corresponds to zero base pressure conditions. The correction to free stream static pressure is constant for given Mach number and so the output is made to change by this calculated amount by adjustment of the K_1 potentiometers.

4.5 C.G. Shift calibration

If the form $J_M M' = J_M M + x_1(\pm J_Z Z)$ is used (section 3.6) it is merely necessary to apply a load at various known positions along the model X-axis, and note the readings of the x_1 potentiometer to achieve zero output M/q.

If the alternative form is used it is necessary to change the output scale setting for each change of the x_1 potentiometer setting. This requires the load to be applied at two positions in succession, first at the proposed reference point, when the output is nulled as before, and secondly as far from this reference as possible, when the gain of the output amplifier must be adjusted to obtain the calculated output corresponding to the moment about the proposed reference point.

5 FACTORS AFFECTING ACCURACY

5.1 Static accuracy

The accuracy aimed at is ±0.1% of the maximum output swing which can be produced by changing the indicator shaft positions from one extremity to the other.

The requirement is for stability and resolution with the need for linearity restricted to a few components. These are the potentiometers fitted to the servo indicators, which have a law accuracy of ±0.1%, and the manometers, ±0.025%, the servo-divider potentiometers, which are within ±0.05% and the operational amplifiers.

The amplifiers used have an open loop gain of about 10^7. Benyon[7] gives the open loop gain, A, of a summing amplifier which is required to achieve a certain fractional error ε as:-

$$A = \frac{1 + \Sigma}{\varepsilon}$$

where Σ is the sum of the closed loop gains for each input to the summer.

Some of the J_F F summing amplifiers have eight inputs, each of unity gain, so in this worst case $\varepsilon = 9 \times 10^{-7}$.

Stability is limited by amplifier drift, temperature changes in summing resistors and stability of reference supplies.

The drift over a long period of the amplifiers is specified less than 100 μV, referred to the summing point. Typically it is claimed to be less than half of this.

Following Howe[8], the output drift e_D of an amplfiier can be related to that at the summing point, e_B, by the expression

$$e_D = (1 + \Sigma)\, e_B \ ,$$

(Σ = sum of closed loop gains).

This gives the output drift of the J_F F amplifiers as 900 μV. The drift in a complete channel is then approximately (1400 G_F + 100) μV which is 0.002% full scale at max G_F or 0.005% at min G_F.

The temperature coefficients of the summing resistors have been specified to be not more than 20 parts per million per degree C. If it so happened that in one channel all the input resistors had limiting coefficients of one sign and all the feedback resistors the opposite sign then 6°C change in ambient temperature could cause the gain of the channel to change by 0.1%. However, this is a remote possibility.

The reference voltage supplies have stability specified as ±0.02%.

The digital voltmeter incorporated in the correction unit has an accuracy of ±0.05% in a range of 19995.

5.2 Dynamic accuracy

The dynamic accuracy requirements for the unit are not at all severe. The input voltages are slowly varying by analogue computing standards if for no other reason than the limitations in dynamic performance of the indicators and manometers.

The only component for which it was thought necessary to specify any dynamic performance was the servo divider. This will follow a change in H_T of 15% of maximum per second with a dynamic error less than 0.1%. In fact this is far in excess of any likely rate of H_T change.

6 PERFORMANCE

Two aspects of performance which are of interest are the success or otherwise of the combined calibration and setting up procedure described in section 4 and the credibility of the outputs under tunnel running conditions.

The crucial part of the former is the interaction cancellation. In order to check this, a typical six-component balance (not embodying the latest design of axial force component) has been calibrated by the method of section 4 and afterwards by the conventional method derived from Ref.5. The normalised interaction matrix programmed in the analogue correction unit by the calibration process was then found. In order to compare the relevant part of it (i.e. excluding the 'X' equation) with the corresponding conventionally found matrix it was necessary to invert and scale it. This process, carried out by digital computer, enforced agreement between the leading terms of the two matrices. The degree of agreement in the other terms then reflected the compatibility of the two calibrations. Each term can of course be represented by the slope or

intercept of a line in the appropriate R_F/W, x plane. A sample of the results is plotted in Figs.8 to 11. In each figure the slope or intercept of one of the lines, as indicated, has been made to agree with the mean value found from the points from the conventional calibration. The intercept or slope of that line, and both slope and intercept of the other line, are freely determined by the calibration technique. The satisfactory agreement between the lines and the points from the conventional calibration shows that the method of section 4 is entirely adequate.

In order to check the remaining performance aspects a tunnel run was made in which the model was traversed through a range of incidence several times and raw and computed data recorded at one degree of incidence intervals on punched paper tape. The raw data was corrected by digital computer, using the balance matrix derived from the analogue machine except in the case of the axial force channel, for which the results of the conventional calibration, which includes small cross product terms, were used. For all components the overall scaling was independently determined by the two different methods.

This check falls short of perfection since to obtain the desired agreement not only must the correction unit performance be up to standard but so also must the servo indicators and balance. It was not possible to freeze the servos during data recording, which occupied twenty seconds per data point. The results then reflect drifts and unsteadiness in indicator readings during the read out period. The datum readings for the two computations were also subject to the same source of discrepancy. Thus we should expect to find random scatter of the differences covering a band corresponding to about 0.2% of servo indicator full scale even if the aerodynamic and/or servo indicator steadiness was of the highest standard to be expected. Also the mean of this band could lie anywhere within the equivalent of ±0.2% of servo full scale from zero if the servo indicators remained within the best expected limits during datum read-out. If the displacement were outside these limits it would be due either to incorrect datum setting on the correction unit or to less than the best balance and servo performance. The second cause is not associated with the correction unit and the former would be condemnatory only if it were due to any difficulty in datum setting. No such difficulty is in fact experienced.

The test was such that at zero incidence all loads except axial force were small so that the outputs were insensitive to the accuracy of scaling. Axial force was sensitive to this and also to the correctness of base pressure compensation. At large incidence the normal force and pitching moment also became large while the three remaining components remained small. Accuracy of scaling would thus be indicated by the absence of any slope in the plots of differences in C_Z and C_M versus incidence. Both conventional and the analogue unit methods of scaling can permit errors which depend on the definition of differences of servo indicator readings at various loads. The further the readings can be spread apart in terms of resulting indicator shaft positions, the better defined is the scaling. In the case of C_M, both methods of calibration utilise the same amount of rotation since moments in both senses are applied, but in the case of C_Z the method for the digital computation required application of loads in one sense only so that less than half the available shaft rotation was used. Thus for this component the method used for the analogue unit scaling is inherently better.

The best results that could be expected then may exhibit a slope within the limits defined by:-

$$\pm \text{load/max. calibration load} \times 0.2\% \text{ Output for full scale servo change,}$$

the discrepancy thus arising being additional to that arising from the previously described source. Limits of best expected agreement as described here have been drawn in Figs.12 to 17.

The presence of non-linear terms due to the particular type of balance design leads to the curvature of the axial force results of Fig.12. There is evidence of scaling errors rather larger than the best expected in the normal force results of Fig.14 but this is in contrast to the pitching moment results of Fig.16 where the scaling error is well within limits. None of the results show any tendency to systematic drift with time.

7 CONCLUSIONS

(1) The analogue unit in the form considered together with the tare correction unit provide corrected data to an order of accuracy consistent with that of the input data so long as no cross product or square term balance interactions are present.

(2) The success of the present equipment leads to the expectation that the extended version of Ref.2 could satisfactorily correct for the non-linear interactions sometimes associated with early designs of aerial force balance. The error in axial component due to neglect of these interactions is not large with the balance used for the evaluation presented here, and considerably smaller errors would be expected in similar circumstances with recent balance designs. The desirability of such an extension is thus open to question.

(3) The dynamic performance of the analogue correction unit would make it suitable for use with input devices considerably faster than the present servo indicators.

(4) The equipment has the considerable advantages of eliminating the delays in production of results associated with off-line digital data correction and enabling the adoption of a simple calibration procedure which eliminates the risk of errors as to the sign or order of magnitude of balance interaction calibration terms.

ACKNOWLEDGEMENT

Acknowledgement is made to Mr. R. Purkiss of Aerodynamics Department who was responsible for the development of the tare correction unit.

Table 2

Comparison of digital and analogue results

No.	C_X		C_Y		C_Z		C_ℓ		C_m		C_n		ΔC_X	ΔC_Y	ΔC_Z	ΔC_ℓ	ΔC_m	ΔC_n	α
	Digital	Analogue	D	A	D	A	D	A	D	A	D	A	D-A	D-A	D-A	D-A	D-A	D-A	
1	-0.326	-0.306	-0.05	-0.05	-0.12	-0.09	0.058	0.045	0.03	-0.05	0.68	0.78	-0.020	0.00	-0.03	0.013	0.08	-0.10	0
2	-0.335	-0.308	-0.06	-0.05	-0.49	-0.46	0.056	0.044	-0.05	-0.16	0.63	0.73	-0.027	-0.01	-0.03	0.012	0.11	-0.10	1
3	-0.338	-0.312	-0.03	-0.06	-0.93	-0.89	0.053	0.042	-0.31	-0.37	0.71	0.80	-0.026	+0.03	-0.04	0.011	0.06	-0.09	2
4	-0.341	-0.318	-0.07	-0.05	-1.26	-1.24	0.050	0.040	-0.50	-0.56	0.64	0.77	-0.023	-0.02	-0.02	0.010	0.06	-0.13	3
5	-0.348	-0.326	-0.04	-0.07	-1.61	-1.60	0.048	0.040	-0.84	-0.93	0.71	0.81	-0.022	+0.03	-0.01	0.008	0.09	-0.10	4
6	-0.359	-0.337	-0.08	-0.04	-2.01	-2.03	0.050	0.040	-1.20	-1.28	0.69	0.80	-0.022	-0.04	+0.02	0.010	0.08	-0.11	5
7	-0.364	-0.338	+0.01	-0.03	-2.45	-2.45	0.052	0.041	-1.56	-1.64	0.70	0.77	-0.026	+0.04	0.00	0.011	0.08	-0.07	6
8	-0.369	-0.347	-0.03	+0.01	-2.83	-2.83	0.049	0.041	-1.94	-1.99	0.73	0.75	-0.022	-0.04	0.00	0.008	0.05	-0.02	7
9	-0.367	-0.351	-0.03	0.00	-3.20	-3.24	0.051	0.040	-2.36	-2.42	0.62	0.76	-0.016	-0.03	+0.04	0.011	0.06	-0.14	8
10	-0.376	-0.357	-0.04	-0.01	-3.64	-3.69	0.048	0.042	-2.81	-2.86	0.67	0.83	-0.019	-0.03	+0.05	0.006	0.05	-0.16	9
11	-0.394	-0.371	-0.05	-0.02	-4.08	-4.12	0.049	0.039	-3.07	-3.17	0.77	0.89	-0.023	-0.03	+0.04	0.010	0.10	-0.12	10
12	-0.392	-0.380	-0.05	-0.02	-4.54	-4.59	0.046	0.037	-3.47	-3.52	0.82	0.88	-0.012	-0.03	+0.05	0.009	0.05	-0.06	11
13	-0.402	-0.388	-0.06	-0.03	-5.01	-5.07	0.043	0.034	-3.76	-3.83	0.78	0.88	-0.014	-0.03	+0.06	0.009	0.07	-0.10	12
14	-0.416	-0.406	-0.04	-0.04	-5.44	-5.52	0.040	00.034	-4.03	-4.10	0.85	0.94	-0.010	0.00	+0.08	0.006	0.07	-0.09	13
15	-0.417	-0.409	-0.07	-0.03	-5.94	-6.05	0.041	0.031	-4.36	-4.43	0.78	0.95	-0.008	-0.04	+0.11	0.010	0.07	-0.07	14
16	-0.416	-0.413	-0.08	-0.05	-6.43	-6.54	0.042	0.032	-4.55	-4.64	0.83	0.90	-0.003	-0.03	+0.11	0.010	0.09	-0.07	15
17	-0.422	-0.426	-0.06	-0.05	-6.96	-7.08	0.043	0.033	-4.88	-4.94	0.85	0.92	+0.004	-0.01	+0.12	0.010	0.06	-0.07	16
18	-0.432	-0.437	-0.03	-0.03	-7.45	-7.57	0.035	0.028	-5.03	-5.06	0.88	1.00	+0.005	0.00	+0.12	0.007	0.03	-0.12	17
19	-0.426	-0.440	-0.04	-0.04	-7.94	-8.09	0.022	0.017	-5.17	-5.22	0.98	1.12	+0.014	0.00	+0.15	0.005	0.05	-0.14	18
20	-0.429	-0.443	-0.05	-0.07	-8.43	-8.59	0.019	0.014	-5.36	-5.39	0.99	1.13	+0.014	+0.02	+0.16	0.005	0.03	-0.14	19
21	-0.431	-0.447	-0.06	-0.06	-8.89	-9.06	0.020	0.014	-5.41	-5.47	0.99	1.14	+0.016	0.00	+0.17	0.006	0.06	-0.15	20
22	-0.424	-0.441	-0.12	-0.09	-8.46	-8.61	0.018	0.014	-5.30	-5.37	0.99	1.19	+0.017	-0.03	+0.15	0.004	0.07	-0.20	19
23	-0.426	-0.438	-0.08	-0.04	-8.00	-8.15	0.022	0.017	-5.05	-5.10	1.01	1.15	+0.012	-0.04	+0.15	0.005	0.05	-0.14	18
24	-0.425	-0.435	-0.10	-0.07	-7.51	-7.65	0.025	0.020	-4.95	-5.02	0.99	1.14	+0.010	-0.03	+0.14	0.003	0.07	-0.15	17
25	-0.416	-0.422	-0.10	-0.08	-7.05	-7.17	0.028	0.024	-4.75	-4.83	0.99	1.13	+0.006	-0.02	+0.12	0.004	0.08	-0.14	16
26	-0.415	-0.414	-0.09	-0.07	-6.52	-6.65	0.032	0.026	-4.48	-4.54	0.98	1.11	-0.001	-0.02	+0.13	0.006	0.06	-0.13	15
27	-0.412	-0.409	-0.08	-0.07	-6.03	-6.14	0.036	0.029	-4.24	-4.27	0.98	1.11	-0.003	-0.01	+0.11	0.007	0.03	-0.13	14
28	-0.408	-0.405	-0.11	-0.10	-5.53	-5.62	0.039	0.031	-3.94	-3.99	0.96	1.06	-0.003	-0.01	+0.09	0.008	0.05	-0.10	13
29	-0.396	-0.390	-0.13	-0.12	-5.07	-5.14	0.042	0.033	-3.60	-3.65	0.99	1.09	-0.006	-0.01	+0.07	0.009	0.05	-0.10	12
30	-0.390	-0.373	-0.12	-0.10	-4.60	-4.64	0.045	0.036	-3.25	-3.34	0.94	1.05	-0.017	-0.02	+0.04	0.009	0.09	-0.11	11
31	-0.384	-0.366	-0.08	-0.06	-4.13	-4.20	0.053	0.041	-2.90	-2.96	0.81	0.93	-0.018	-0.02	+0.07	0.012	0.06	-0.12	10
32	-0.371	-0.354	-0.07	-0.08	-3.70	-3.74	0.052	0.044	-2.60	-2.67	0.81	0.93	-0.017	+0.01	+0.04	0.008	0.07	-0.12	9
33	-0.361	-0.344	-0.07	-0.07	-3.29	-3.31	0.055	0.045	-2.18	-2.24	0.81	0.90	-0.017	0.00	+0.02	0.010	0.06	-0.09	8
34	-0.364	-0.341	-0.06	-0.10	-2.88	-2.89	0.057	0.046	-1.72	-1.77	0.81	0.92	-0.023	+0.04	+0.01	0.011	0.05	-0.11	7
35	-0.360	-0.377	-0.09	-0.06	-2.48	-2.48	0.056	0.046	-1.40	-1.46	0.79	0.92	-0.023	-0.03	0.00	0.010	0.06	-0.13	6
36	-0.359	-0.337	-0.08	-0.07	-2.04	-2.06	0.059	0.047	-1.05	-1.10	0.79	0.92	-0.022	-0.01	+0.02	0.012	0.05	-0.13	5
37	-0.351	-0.328	-0.08	-0.06	-1.64	-1.63	0.061	0.049	-0.68	-0.72	0.79	0.92	-0.023	-0.02	-0.01	0.012	0.04	-0.13	4
38	-0.348	-0.321	-0.07	-0.07	-1.29	-1.28	0.059	0.050	-0.35	-0.43	0.79	0.93	-0.027	0.00	-0.01	0.009	0.08	-0.14	3
39	-0.346	-0.321	-0.07	-0.09	-0.95	-0.91	0.062	0.051	-0.11	-0.18	0.84	0.93	-0.025	+0.02	-0.04	0.011	0.07	-0.09	2
40	-0.343	-0.318	-0.06	-0.07	-0.55	-0.52	0.064	0.053	+0.16	+0.07	0.89	0.97	-0.025	+0.01	-0.03	0.011	0.09	-0.08	1

Table 2 (Contd)

No.	C_X		C_Y		C_Z		C_ℓ		C_m		C_n		ΔC_X	ΔC_Y	ΔC_Z	ΔC_ℓ	ΔC_m	ΔC_n	α
	Digital	Analogue	D	A	D	A	D	A	D	A	D	A	D-A	D-A	D-A	D-A	D-A	D-A	
41	-0.333	-0.317	-0.09	-0.09	-0.15	-0.11	+0.063	+0.052	+0.19	+0.11	+0.86	+0.98	-0.016	0.00	-0.04	+0.011	+0.08	-0.12	0
42	-0.336	-0.318	-0.12	-0.10	+0.22	+0.23	+0.065	+0.053	+0.42	+0.35	+0.84	+0.97	-0.018	-0.02	-0.01	+0.012	+0.07	-0.13	-1
43	-0.341	-0.327	-0.11	-0.08	+0.56	+0.58	+0.063	+0.053	+0.65	+0.57	+0.84	+0.91	-0.014	-0.03	-0.02	+0.010	+0.08	-0.07	-2
44	-0.347	-0.334	-0.07	-0.08	+0.93	+0.98	+0.070	+0.055	+0.88	+0.80	+0.86	+0.97	-0.013	+0.01	-0.05	+0.015	+0.08	-0.11	-3
45	-0.357	-0.315	-0.0[illegible]	-0.09	+0.94	+0.99	+0.066	+0.044	-0.10	+0.88	+0.29	+1.04	-0.042	+0.03	-0.05	+0.022	-0.98	-0.75	-4
46	-0.331	-0.317	-0.11	-0.06	+0.94	+0.99	+0.061	+0.049	+0.98	+0.89	+0.89	+1.02	-0.014	-0.05	-0.05	+0.012	+0.09	-0.13	-3
47	-0.343	-0.326	-0.07	-0.07	+1.31	+1.36	+0.055	+0.046	+1.25	+1.14	+0.91	+1.07	-0.017	0.00	-0.05	+0.009	+0.11	-0.16	-4
48	-0.347	-0.333	-0.06	-0.08	+1.66	+1.71	+0.057	+0.047	+1.64	+1.53	+0.91	+1.05	-0.014	+0.02	-0.05	+0.010	+0.11	-0.14	-5
49	-0.352	-0.341	-0.06	-0.06	+2.12	+2.17	+0.056	+0.044	+1.93	+1.85	+0.91	+1.08	-0.011	0.00	-0.05	+0.012	+0.08	-0.17	-6
50	-0.357	-0.345	-0.05	-0.06	+2.53	+2.61	+0.049	+0.040	+2.39	+2.31	+0.96	+1.08	-0.012	+0.01	-0.08	+0.009	+0.08	-0.12	-7
51	-0.364	-0.354	-0.08	-0.05	+2.94	+3.04	+0.047	+0.039	+2.76	+2.69	+0.90	+1.08	-0.010	-0.03	-0.10	+0.008	+0.07	-0.18	-8
52	-0.368	-0.362	-0.07	-0.05	+3.40	+3.48	+0.051	+0.040	+3.11	+3.03	+0.95	+1.08	-0.006	-0.02	-0.08	+0.011	+0.08	-0.13	-9.
53	-0.378	-0.369	-0.03	-0.04	+3.81	+3.89	+0.049	+0.040	+3.57	+3.49	+0.97	+1.09	-0.009	+0.01	-0.08	+0.009	+0.08	-0.12	-10
54	-0.393	-0.385	-0.03	-0.00	+4.24	+4.35	+0.048	+0.037	+3.87	+3.80	+0.97	+1.09	-0.008	-0.03	-0.11	+0.011	+0.07	-0.12	-11
55	-0.394	-0.392	-0.02	-0.03	+4.71	+4.82	+0.042	+0.034	+4.22	+4.15	+0.97	+1.11	-0.002	+0.01	-0.11	+0.008	+0.07	-0.14	-12
56	-0.403	-0.402	-0.05	-0.02	+5.24	+5.35	+0.045	+0.036	+4.55	+4.45	+1.00	+1.13	-0.001	-0.03	-0.11	+0.009	+0.10	-0.13	-13
57	-0.408	-0.411	-0.04	-0.01	+5.74	+5.26	+0.044	+0.036	+4.84	+4.74	+1.00	+1.13	+0.003	-0.03	-0.12	+0.008	+0.10	-0.13	-14
58	-0.406	-0.410	-0.03	+0.03	+6.23	+6.36	+0.052	+0.040	+5.13	+5.04	+0.99	+1.15	+0.004	-0.06	-0.13	+0.012	+0.09	-0.16	-15
59	-0.408	-0.422	-0.02	+0.01	+6.72	+6.86	+0.051	+0.040	+5.32	+5.20	+0.99	+1.15	+0.014	-0.03	-0.14	+0.011	+0.12	-0.16	-16
60	-0.411	-0.429	-0.02	+0.01	+7.24	+7.41	+0.050	+0.040	+5.45	+5.34	+0.99	+1.13	+0.018	-0.03	-0.17	+0.010	+0.11	-0.14	-17
61	-0.410	-0.432	+0.03	+0.02	+7.67	+7.85	+0.035	+0.026	+5.71	+5.56	+0.91	+1.02	+0.022	+0.01	-0.18	+0.009	+0.15	-0.11	-18
62	-0.411	-0.457	0.00	+0.03	+8.16	+8.38	+0.034	+0.027	+5.75	+5.63	+0.98	+1.08	+0.026	-0.03	-0.22	+0.007	+0.12	-0.10	-19
63	-0.411	-0.456	-0.03	-0.05	+8.63	+8.79	+0.019	+0.016	+5.95	+5.79	+1.16	+1.26	+0.045	+0.02	-0.16	+0.003	+0.16	-0.10	-20
64	-0.415	-0.445	-0.04	-0.03	+8.10	+8.29	+0.011	+0.008	+5.72	+5.62	++1.11	+1.25	+0.030	-0.01	-0.19	+0.003	+0.10	-0.14	-19
65	-0.416	-0.438	-0.01	-0.03	+7.64	+7.81	+0.008	+0.005	+5.57	+5.45	+1.09	+1.20	+0.022	+0.02	-0.17	+0.003	+0.12	-0.11	-18
66	-0.413	-0.436	-0.05	-0.02	+7.24	+7.38	+0.009	+0.008	+5.35	+5.23	+1.02	+1.15	+0.023	-0.03	-0.14	+0.001	+0.12	-0.13	-17
67	-0.414	-0.441	-0.03	-0.02	+6.63	+6.79	+0.014	+0.011	+5.25	+5.15	+1.09	+1.19	+0.027	-0.01	-0.16	+0.003	+0.10	-0.10	-16
68	-0.407	-0.417	-0.07	-0.03	+6.17	+6.29	+0.015	+0.014	+4.95	+4.86	+1.02	+1.19	+0.010	-0.04	-0.12	+0.001	+0.09	-0.17	-15
69	-0.414	-0.415	-0.08	-0.04	+5.64	+5.77	+0.016	+0.010	+4.77	+4.65	+1.03	+1.16	+0.001	-0.04	-0.13	+0.006	+0.12	-0.13	-14
70	-0.406	-0.409	-0.05	-0.05	+5.15	+5.27	+0.013	+0.009	+4.39	+4.27	+1.05	+1.16	+0.003	0.00	-0.12	+0.004	+0.12	-0.11	-13
71	-0.409	-0.404	-0.06	-0.07	+4.63	+4.78	+0.009	+0.009	+4.09	+3.96	+1.00	+1.16	-0.005	+0.01	-0.10	0.000	+0.13	-0.16	-12
72	-0.404	-0.396	-0.06	-0.06	+4.18	+4.28	+0.010	+0.010	+3.70	+3.60	+1.00	+1.15	-0.008	0.00	-0.10	0.000	+0.10	-0.15	-11
73	-0.394	-0.389	-0.07	-0.05	+3.72	+3.81	+0.012	+0.012	+3.36	+3.24	+1.00	+1.14	-0.005	-0.02	-0.09	0.000	+0.12	-0.14	-10
74	-0.370	-0.370	-0.08	-0.05	+3.31	+3.38	+0.013	+0.011	+2.99	+2.87	+1.00	+1.13	0.000	-0.03	-0.07	+0.002	+0.12	-0.13	-9
75	-0.386	-0.356	-0.08	-0.06	+2.87	+2.93	+0.015	+0.011	+2.49	+2.40	+0.99	+1.12	-0.020	-0.02	-0.06	+0.004	+0.09	-0.13	-8
76	-0.373	-0.366	-0.09	-0.09	+2.50	+2.57	+0.012	+0.012	+2.16	+2.06	+0.99	+1.14	-0.007	0.00	-0.07	0.000	+0.10	-0.15	-7
77	-0.373	-0.360	-0.09	-0.09	+2.09	+2.12	+0.014	+0.012	+1.75	+1.66	+0.99	+1.12	-0.013	0.00	-0.03	+0.002	+0.09	-0.13	-6
78	-0.366	-0.355	-0.10	-0.09	+1.65	+1.70	+0.020	+0.015	+1.35	+1.25	+0.99	+1.11	-0.011	-0.01	-0.05	+0.005	+0.10	-0.12	-5
79	-0.362	-0.349	-0.11	-0.09	+1.31	+1.34	+0.018	+0.013	+1.11	+0.99	+0.99	+1.14	-0.013	-0.02	-0.03	+0.002	+0.12	-0.15	-4
80	-0.358	-0.342	-0.11	-0.11	+0.93	+0.96	+0.024	+0.020	+0.69	+0.61	+0.99	+1.13	-0.016	0.00	-0.03	+0.004	+0.08	-0.14	-3

Table 2 (Contd)

No.	C_X		C_Y		C_Z		C_ℓ		C_m		C_n		ΔC_X	ΔC_Y	ΔC_Z	ΔC_ℓ	ΔC_m	ΔC_n	α
	Digital	Analogue	D	A	D	A	D	A	D	A	D	A	D-A	D-A	D-A	D-A	D-A	D-A	
81	-0.353	-0.337	-0.08	-0.10	+0.56	+0.57	+0.027	+0.023	+0.45	+0.39	+1.01	+1.13	-0.016	+0.02	-0.01	+0.004	+0.06	-0.12	-2
82	-0.351	-0.333	-0.09	-0.11	+0.19	+0.21	+0.028	+0.022	+0.23	+0.12	+1.01	+1.14	-0.018	+0.02	-0.02	+0.006	+0.11	-0.13	-1
83	-0.344	-0.328	-0.13	-0.11	-0.21	-0.17	+0.030	+0.023	+0.06	-0.01	+0.99	+1.14	-0.016	-0.02	-0.04	+0.007	+0.07	-0.15	0
84	-0.368	-0.345	-0.09	-0.09	-0.22	-0.19	+0.049	+0.041	-0.04	-0.12	+0.86	+0.99	-0.023	0.00	-0.03	+0.008	+0.08	-0.13	0
85	-0.373	-0.347	-0.10	-0.11	-0.56	-0.54	+0.051	+0.041	-0.18	-0.23	+0.86	+0.97	-0.026	+0.01	-0.02	+0.010	+0.05	-0.11	1
86	-0.372	-0.348	-0.07	-0.08	-0.96	-0.96	+0.048	+0.039	-0.30	-0.40	+0.89	+0.98	-0.024	+0.01	0.00	+0.009	+0.10	-0.09	2
87	-0.374	-0.349	-0.07	-0.08	-1.36	-1.35	+0.045	+0.037	-0.47	-0.54	+0.84	+0.93	-0.025	+0.01	-0.01	+0.008	+0.07	-0.09	3
88	-0.381	-0.355	-0.08	-0.06	-1.67	-1.69	+0.052	+0.041	-0.82	-0.90	+0.79	+0.90	-0.026	-0.02	+0.02	+0.011	+0.08	-0.11	4
89	-0.381	-0.358	-0.05	-0.01	-2.08	-2.09	+0.049	+0.040	-1.18	-0.25	+0.76	+0.88	-0.023	-0.04	+0.01	+0.009	+0.07	-0.12	5
90	-0.384	-0.365	-0.02	-0.01	-2.48	-2.57	+0.051	+0.043	-1.50	-1.57	+0.73	+0.86	-0.019	-0.01	+0.09	+0.008	+0.07	-0.13	6
91	-0.390	-0.373	-0.03	-0.01	-2.88	-2.90	+0.048	+0.043	-1.82	-1.91	+0.78	+0.88	-0.017	-0.02	+0.02	+0.005	+0.09	-0.10	7
92	-0.407	-0.386	+0.03	0.00	-3.26	-3.32	+0.055	+0.043	-2.25	-2.31	+0.77	+0.87	-0.021	+0.03	+0.06	+0.012	+0.06	-0.10	8
93	-0.409	-0.393	-0.04	-0.01	-3.70	-3.74	+0.052	+0.042	-2.69	-2.76	+0.73	+0.88	-0.016	-0.03	+0.04	+0.010	+0.07	-0.15	9
94	-0.415	-0.398	+0.02	+0.03	-4.13	-4.20	+0.049	+0.040	-3.01	-3.08	+0.82	+0.87	-0.017	-0.01	+0.07	+0.009	+0.07	-0.05	10
95	-0.436	-0.415	+0.01	0.00	-4.57	-4.64	+0.051	+0.040	-3.41	-3.45	+0.77	+0.89	-0.021	+0.01	+0.07	+0.011	+0.04	-0.11	11
96	-0.437	-0.426	+0.01	+0.02	-5.07	-5.14	+0.047	+0.037	-3.70	-3.75	+0.77	+0.88	-0.011	-0.01	+0.07	+0.010	+0.05	-0.11	12
97	-0.445	-0.437	+0.03	-0.01	-5.53	-5.60	+0.049	+0.039	-4.00	-4.06	+0.79	+0.87	-0.008	+0.04	+0.07	+0.010	+0.06	-0.08	13
98	-0.450	-0.446	-0.01	-0.01	-6.02	-6.13	+0.045	+0.038	-4.33	-4.38	+0.77	+0.89	-0.004	0.00	+0.11	+0.007	+0.05	-0.12	14
99	-0.454	-0.453	+0.02	0.00	-6.49	-6.60	+0.042	+0.034	-4.58	-4.61	+0.79	+0.95	-0.001	+0.02	+0.11	+0.008	+0.03	-0.16	15
100	-0.454	-0.458	-0.03	-0.02	-7.01	-7.16	+0.038	+0.031	-4.86	-4.90	+0.87	+0.98	+0.004	-0.01	+0.15	+0.007	+0.04	-0.11	16
101	-0.453	-0.462	-0.04	+0.01	-7.50	-7.64	+0.035	+0.030	-5.00	-5.04	+0.88	+1.01	+0.009	-0.05	+0.14	+0.005	+0.04	-0.13	17
102	-0.458	-0.469	-0.01	-0.02	-7.96	-8.12	+0.031	+0.026	-5.16	-5.21	+0.85	+0.96	+0.011	+0.01	+0.16	+0.005	+0.05	-0.11	18
103	-0.455	-0.472	-0.02	-0.03	-8.49	-8.62	+0.028	+0.023	-5.34	-5.38	+0.91	+1.01	+0.017	-0.01	+0.13	+0.005	+0.04	-0.10	19
104	-0.477	-0.483	-0.03	-0.01	-8.94	-8.10	+0.033	+0.030	-5.39	-5.44	+0.91	+1.02	+0.006	-0.02	+0.16	+0.003	+0.05	-0.10	20
105	-0.449	-0.468	+0.05	+0.05	-8.52	-8.66	+0.028	+0.023	-5.28	-5.36	+0.90	+1.04	+0.019	0.00	+0.14	+0.005	+0.08	-0.14	19
106	-0.452	-0.465	+0.05	+0.02	-8.05	-8.20	+0.031	+0.025	-5.04	-5.09	+0.90	+1.01	+0.013	+0.02	+0.15	+0.005	+0.05	-0.11	18
107	-0.448	-0.457	-0.04	+0.02	-7.59	-7.73	+0.038	+0.030	-4.92	-4.98	+0.88	+1.02	+0.009	-0.03	+0.15	+0.008	+0.06	-0.14	17
108	-0.446	-0.450	+0.01	+0.03	-7.10	-7.22	+0.042	+0.033	-4.69	-4.74	+0.85	+0.99	+0.004	-0.02	+0.12	+0.009	+0.05	-0.14	16
109	-0.450	-0.449	+0.02	-0.02	-6.58	-6.70	+0.046	+0.038	-4.46	-4.51	+0.80	+0.90	-0.001	+0.04	+0.12	+0.008	+0.05	-0.10	15
110	-0.445	-0.439	+0.02	+0.02	-6.08	-6.19	+0.054	+0.044	-4.17	-4.24	+0.90	+0.91	-0.006	0.00	+0.11	+0.010	+0.07	-0.01	14
111	-0.436	-0.427	0.00	+0.03	-5.56	-5.66	+0.058	+0.046	-3.94	-3.98	+0.32	+0.91	-0.009	-0.02	+0.10	+0.012	+0.04	-0.09	13
112	-0.429	-0.420	0.00	+0.01	-5.09	-5.16	+0.056	+0.045	-3.59	-3.64	+0.82	+0.94	-0.009	-0.01	+0.07	+0.011	+0.05	-0.12	12
113	-0.418	-0.412	-0.02	+0.01	-4.63	-4.70	+0.055	+0.046	-3.24	-3.33	+0.80	+0.87	-0.006	-0.03	+0.07	+0.009	+0.09	-0.07	11
114	-0.405	-0.389	-0.05	-0.01	-4.19	-4.25	+0.058	+0.049	-2.84	-2.92	+0.73	+0.87	-0.016	-0.04	+0.06	+0.009	+0.08	-0.14	10
115	-0.407	-0.384	-0.01	+0.04	-3.76	-3.80	+0.061	+0.050	-2.58	-2.63	+0.75	+0.85	-0.023	-0.05	+0.04	+0.011	+0.05	-0.10	9
116	-0.392	-0.374	-0.30	+0.01	-3.35	-3.37	+0.059	+0.047	-2.12	-2.19	+0.73	+0.83	-0.018	-0.04	+0.02	+0.012	+0.07	-0.10	8
117	-6.295	-0.364	-0.31	-0.01	-3.71	-2.96	+0.616	+0.048	-17.83	-1.72	+7.89	+0.84							7
118	-0.374	-0.353	-0.02	0.00	-2.51	-2.53	+0.060	+0.050	-1.40	-1.45	+0.73	+0.83	-0.021	-0.02	+0.02	+0.010	+0.05	-0.10	6
119	-0.377	-0.352	-0.02	-0.05	-2.10	-2.11	+0.063	+0.052	-1.03	-1.09	+0.78	+0.84	-0.025	+0.03	+0.01	+0.011	+0.06	-0.06	5
120	-0.367	-0.347	-0.08	-0.07	-1.69	-1.69	+0.066	+0.053	-0.61	-0.69	+0.74	+0.88	-0.020	-0.01	0.00	+0.013	+0.08	-0.14	4

Table 2 (Contd)

No.	C_X		C_Y		C_Z		C_ℓ		C_m		C_n		ΔC_X	ΔC_Y	ΔC_Z	ΔC_ℓ	ΔC_m	ΔC_n	α
	Digital	Analogue	D	A	D	A	D	A	D	A	D	A	D-A	D-A	D-A	D-A	D-A	D-A	
121	-0.369	-0.343	-0.07	-0.07	-1.32	-1.31	+0.064	+0.053	-0.34	-0.41	+0.79	+0.90	-0.026	0.00	-0.01	+0.011	+0.07	-0.11	3
122	-0.364	-0.344	-0.07	-0.07	-0.98	-0.95	+0.066	+0.055	-0.05	-0.11	+0.79	+0.89	-0.020	0.00	-0.03	+0.011	+0.06	-0.10	2
123	-0.359	-0.333	-0.09	-0.07	-0.58	-0.55	+0.069	+0.056	+0.17	+0.09	+0.77	+0.89	-0.026	-0.02	-0.03	+0.013	+0.08	-0.12	1
124	-0.348	-0.331	-0.09	-0.09	-0.21	-0.17	+0.071	+0.057	+0.25	+0.16	+0.76	+0.87	-0.017	0.00	-0.04	+0.014	+0.09	-0.11	0
125	-0.335	-0.319	-0.09	-0.09	-0.21	-0.17	+0.058	+0.046	+0.35	+0.26	+0.92	+1.06	-0.016	0.00	-0.04	+0.012	+0.09	-0.14	0
126	-0.340	-0.320	-0.09	-0.10	+0.17	+0.19	+0.060	+0.047	+0.63	+0.52	+0.92	+1.06	-0.020	+0.01	-0.02	+0.013	+0.11	-0.14	-1
127	-0.345	-0.324	-0.08	-0.09	+0.54	+0.55	+0.058	+0.046	+0.76	+0.68	+0.91	+1.04	-0.021	+0.01	-0.01	+0.012	+0.08	-0.13	-2
128	-0.349	-0.331	-0.11	-0.09	+0.91	+0.95	+0.056	+0.044	+1.04	+0.95	+0.89	+1.05	-0.018	-0.02	-0.04	+0.012	+0.09	-0.16	-3
129	-0.359	-0.344	-0.07	-0.08	+1.28	+1.32	+0.050	+0.042	+1.26	+1.20	+0.91	+1.06	-0.015	+0.01	-0.04	+0.008	+0.06	-0.15	-4
130	-0.363	-0.349	-0.10	-0.07	+1.63	+1.68	+0.047	+0.040	+1.70	+1.65	+0.89	+1.11	-0.014	-0.03	-0.05	+0.007	+0.05	-0.22	-5
131	-0.367	-0.354	-0.09	-0.07	+2.06	+2.12	+0.046	+0.038	+2.00	+1.95	+0.99	+1.12	-0.013	-0.02	-0.06	+0.008	+0.05	-0.13	-6
132	-0.374	-0.361	-0.09	-0.06	+2.50	+2.55	+0.044	+0.037	+2.41	+2.35	+0.95	+1.11	-0.013	-0.03	-0.05	+0.010	+0.06	-0.16	-7
133	-0.378	-0.366	-0.08	-0.06	+2.91	+2.98	+0.047	+0.037	+2.82	+2.77	+0.95	+1.13	-0.012	-0.02	-0.07	+0.010	+0.05	-0.18	-8
134	-0.386	-0.375	-0.08	-0.05	+3.34	+3.42	+0.041	+0.035	+3.22	+3.13	+1.00	+1.12	-0.011	-0.03	-0.08	+0.006	+0.09	-0.12	-9
135	-0.394	-0.390	-0.07	-0.04	+3.72	+3.83	+0.035	+0.029	+3.65	+3.58	+1.00	+1.12	-0.004	-0.03	-0.11	+0.006	+0.07	-0.12	-10
136	-0.404	-0.400	-0.06	-0.04	+4.22	+4.30	+0.038	+0.031	+4.03	+3.93	+1.00	+1.15	-0.004	-0.02	-0.08	+0.007	+0.10	-0.15	-11
137	-0.409	-0.408	-0.06	-0.04	+4.68	+4.78	+0.037	+0.031	+4.33	+4.25	+1.00	+1.15	-0.001	-0.02	-0.10	+0.006	+0.08	-0.15	-12
138	-0.420	-0.420	-0.05	0.00	+5.15	+5.27	+0.040	+0.031	+4.62	+4.53	+1.00	+1.16	0.000	-0.05	-0.12	+0.009	+0.09	-0.16	-13
139	-0.427	-0.430	-0.04	-0.04	+5.64	+5.78	+0.039	+0.033	+4.96	+4.86	+1.00	+1.14	+0.003	0.00	-0.14	+0.006	+0.10	-0.14	-14
140	-0.426	-0.436	-0.03	-0.02	+6.17	+6.29	+0.047	+0.037	+5.29	+5.17	+1.00	+1.13	+0.010	-0.01	-0.12	+0.010	+0.12	-0.13	-15
141	-0.428	-0.444	-0.03	-0.02	+6.63	+6.77	+0.051	+0.038	+5.39	+5.30	+0.99	+1.13	+0.016	-0.01	-0.14	+0.013	+0.09	-0.14	-16
142	-0.437	-0.453	-0.02	0.00	+7.21	+7.35	+0.050	+0.040	+5.50	+5.42	+0.99	+1.13	+0.016	-0.02	-0.14	+0.010	+0.08	-0.14	-17
143	-0.435	-0.456	-0.01	-0.01	+7.64	+7.80	+0.049	+0.039	+5.71	+5.59	+0.99	+1.11	+0.021	0.00	-0.16	+0.010	+0.12	-0.12	-18
144	-0.432	-0.459	-0.04	-0.01	+8.10	+8.27	+0.047	+0.038	+5.77	+5.67	+1.01	+1.18	+0.027	-0.03	-0.17	+0.009	+0.10	-0.17	-19
145	-0.423	-0.474	-0.03	-0.02	+8.59	+8.75	+0.055	+0.044	+6.01	+5.87	+1.06	+1.18	+0.051	-0.01	-0.16	+0.011	+0.14	-0.12	-20
146	-0.459	-0.464	-0.07	-0.06	+8.07	+8.22	+0.047	+0.036	+5.83	+5.69	+1.04	+1.16	+0.005	-0.01	-0.15	+0.011	+0.14	-0.12	-19
147	-0.441	-0.464	-0.08	-0.06	+7.61	+7.74	+0.044	+0.036	+5.68	+5.56	+0.94	+1.09	+0.023	-0.02	-0.13	+0.008	+0.12	-0.15	-18
148	-0.443	-0.454	-0.05	-0.04	+7.12	+7.27	+0.045	+0.035	+5.44	+5.53	+0.92	+1.09	+0.011	-0.01	-0.15	+0.010	+0.11	-0.17	-17
149	-0.440	-0.448	-0.06	-0.04	+6.59	+6.74	+0.046	+0.036	+5.26	+5.17	+0.87	+1.04	+0.008	-0.02	-0.15	+0.010	+0.09	-0.17	-16
150	-0.434	-0.444	-0.03	-0.04	+6.13	+6.27	+0.047	+0.039	+5.06	+4.95	+0.89	+1.04	+0.010	+0.01	-0.13	+0.008	+0.11	-0.15	-15
151	-0.435	-0.441	-0.04	-0.04	+5.61	+5.73	+0.048	+0.036	+4.78	+4.71	+0.89	+0.99	+0.006	0.00	-0.12	+0.012	+0.07	-0.10	-14
152	-0.431	-0.432	-0.05	-0.03	+5.11	+5.21	+0.040	+0.034	+4.44	+4.36	+0.85	+0.99	+0.001	-0.02	-0.10	+0.016	+0.08	-0.14	-13
153	-0.428	-0.416	-0.05	-0.05	+4.59	+4.71	+0.041	+0.034	+4.16	+4.05	+0.85	+1.01	-0.012	0.00	-0.12	+0.007	+0.11	-0.16	-12
154	-0.411	-0.407	-0.06	-0.05	+4.15	+4.25	+0.042	+0.032	+3.76	+3.64	+0.85	+0.97	-0.004	-0.01	-0.10	+0.010	+0.12	-0.12	-11
155	-0.414	-0.400	-0.07	-0.07	+3.68	+3.78	+0.043	+0.037	+3.41	+3.31	+0.85	+0.98	-0.014	0.00	-0.10	+0.006	+0.10	-0.13	-10
156	-0.400	-0.392	-0.07	-0.07	+3.25	+3.33	+0.050	+0.039	+3.01	+2.92	+0.85	+0.99	-0.008	0.00	-0.08	+0.011	+0.09	-0.14	-9
157	-0.399	-0.386	-0.08	-0.08	+2.84	+2.91	+0.047	+0.038	+2.60	+2.48	+0.84	+0.97	-0.013	0.00	-0.07	+0.009	+0.12	-0.13	-8
158	-0.391	-0.383	-0.08	-0.09	+2.46	+2.54	+0.049	+0.038	+2.17	+2.09	+0.84	+0.96	-0.008	+0.01	-0.08	+0.011	+0.08	-0.12	-7
159	-0.380	-0.375	-0.09	-0.10	+2.03	+2.07	+0.055	+0.043	+1.82	+1.70	+0.84	+0.97	-0.005	+0.01	-0.04	+0.012	+0.12	-0.13	-6
160	-0.382	-0.362	-0.10	-0.09	+1.65	+1.68	+0.052	+0.044	+1.40	+1.29	+0.84	+0.97	-0.020	-0.01	-0.03	+0.008	+0.11	-0.13	-5

SYMBOLS

X, Y, Z	force components along x, y, z axes
L, M, N	moment components about x, y, z axes
Ox, y, z	body fixed axes system
σ	angle of incidence of model
λ	angle of roll of model
ε	misalignment due to balance imperfection
w	model weight
x_g	distance of model C.G. from origin
Pb	base pressure
H_T	stagnation pressure of free stream
E	servo indicator shaft position
R	change of position from datum $(E - E_o)$
F	generalisation for X, Y, Z, L, M, N
a, b → f	calibration constants
k	balance temperature coefficient
J	scaling factor, inverse of leading coefficient in balance equation
K	scaling factor, pressures
x	distance of C.G. shift
G	gain of output amplifier
V_S	standard for servo divider
q	kinetic pressure
Σ	sum of closed loop gains of summing amplifier
A_1, A_2, B_1, B_2	sting bending coefficients
$\Delta\alpha$	sting deflection angle in the xz plane
$\Delta\beta$	sting deflection angle in the xy plane

Suffices

o	refers to datum conditions
A	refers to first, second or third temperature measurement channel
F	generalisation for X, Y, Z, L, M, N
X, Y, Z, L, M, N	quantities related to corresponding force or moment channel

REFERENCES

No.	Author	Title, etc.
1	J.R. Anderson	A note on the use of strain gauges in wind tunnel balances. AGARD Memo AG10/M6, January 1954
2	L J. Beecham W.L. Walters D.W. Partridge	Proposals for an integrated wind-tunnel flight dynamics simulator system A.R.C. C.P. 789, November 1962
3	T.F. Midwood R.W. Hayward	An automatic self balancing capsule manometer. R.A.E. Tech Note 2382 (A.R.C. C.P. 231, A.R.C. 18167), July 1955
4	G.F. Moss D.G. Payne	A compact design of six component internal strain gauge balance. R.A.E. Tech Note Aero 2764, July 1961
5	J.R. Anderson	A method for calibrating a wind tunnel rear sting balance. R.A.E. Tech Note Aero 2299, March 1954
6	B.E. Pecover	The new model attitude control system developed for the R.A.E. No.19 wind-tunnel. To be published
7	P.R. Benyon	A new D.C. amplifier for general use in electronic analogue computers. R.A.E. Tech Note G.W.426, August 1956
8	R.M. Howe	Design fundamentals of analogue computer components. Ch.2 para 2.6. D. Van Nostrand Company Inc., Princeton N.J.

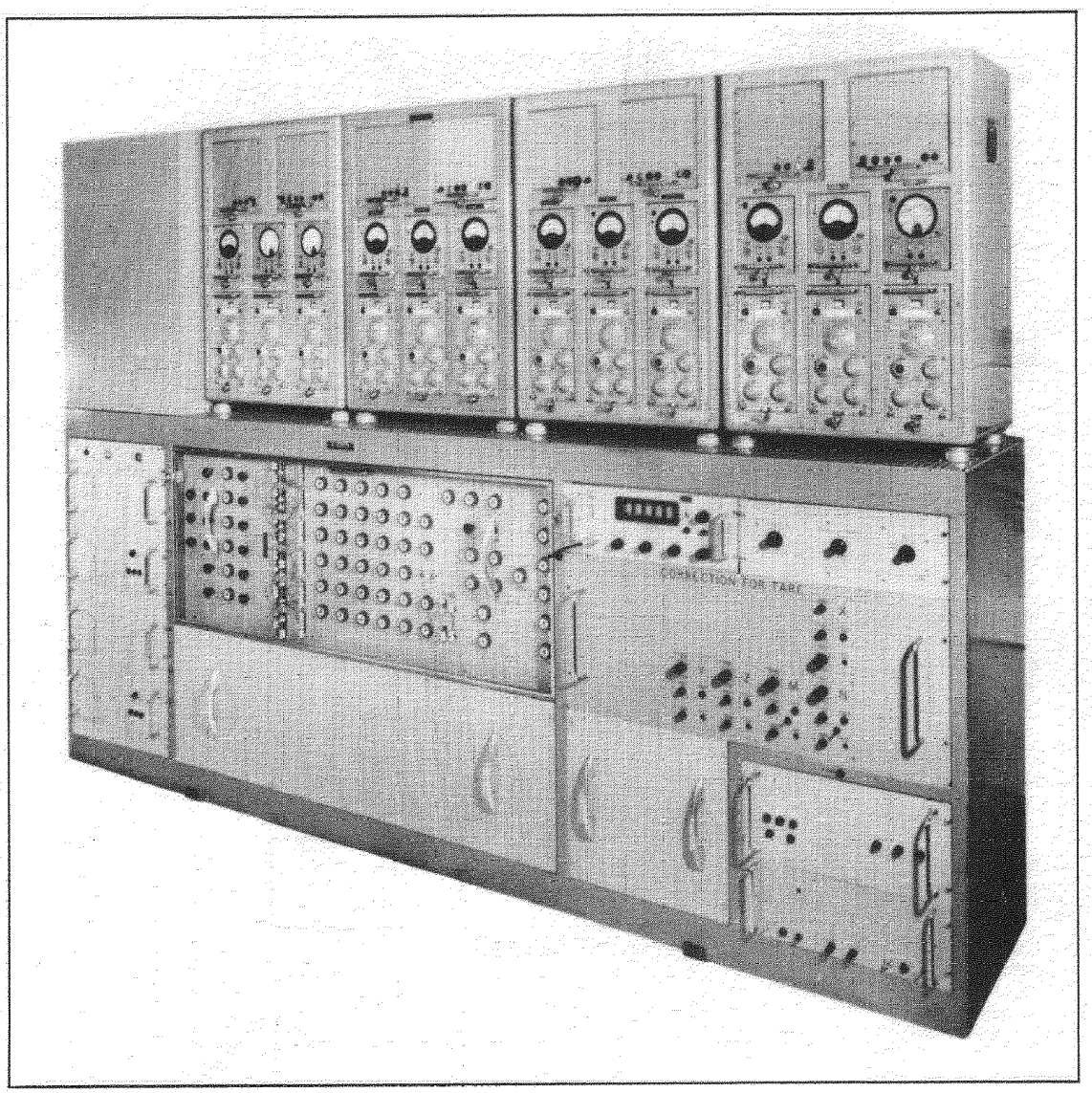

Fig.1 Assembled analogue correction unit, tare correction unit and strain gauge indicators

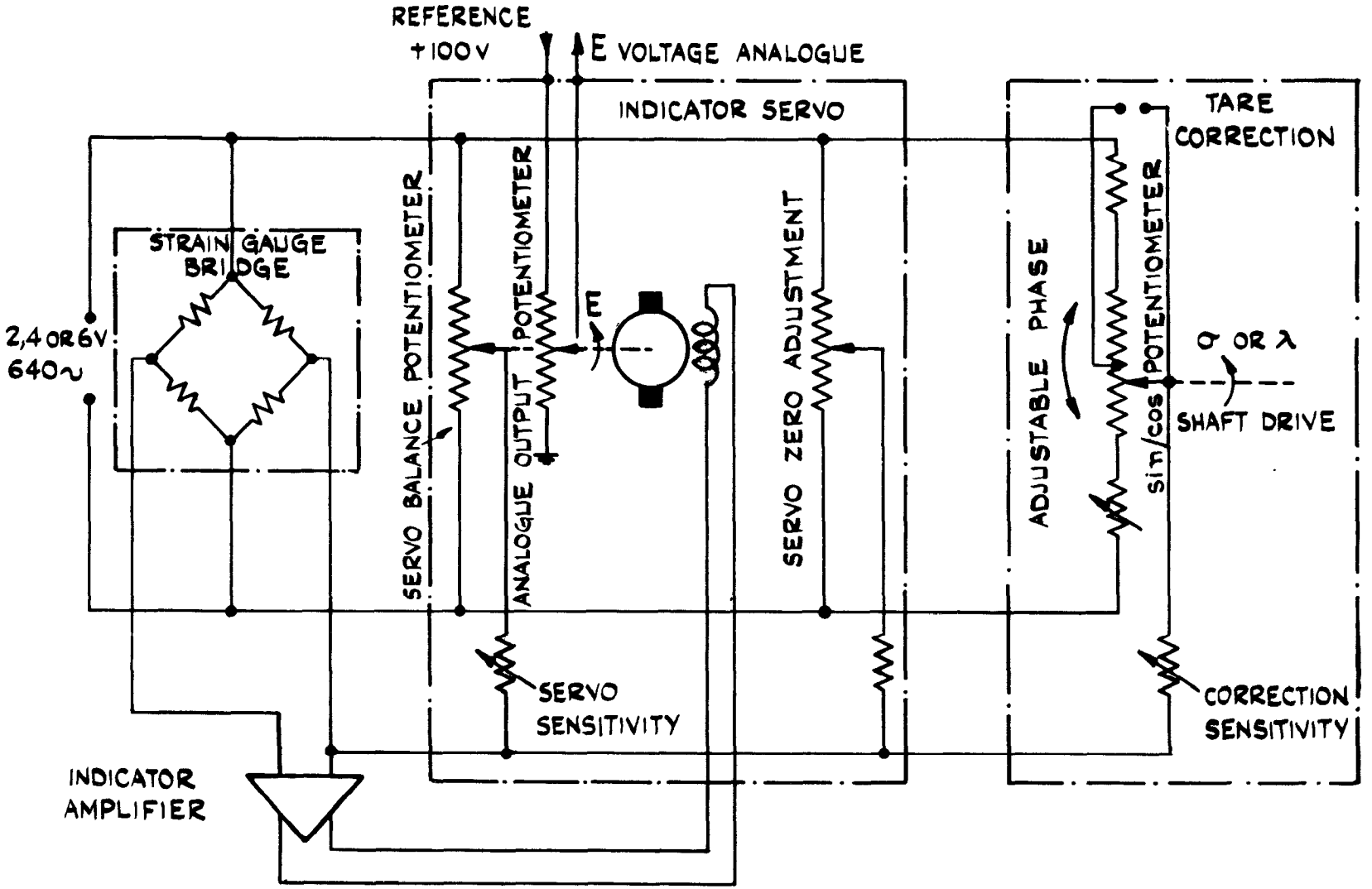

FIG 2 SCHEMATIC DIAGRAM OF ONE CHANNEL OF STRAIN GAUGE BALANCE, INDICATOR, AND TARE CORRECTION.

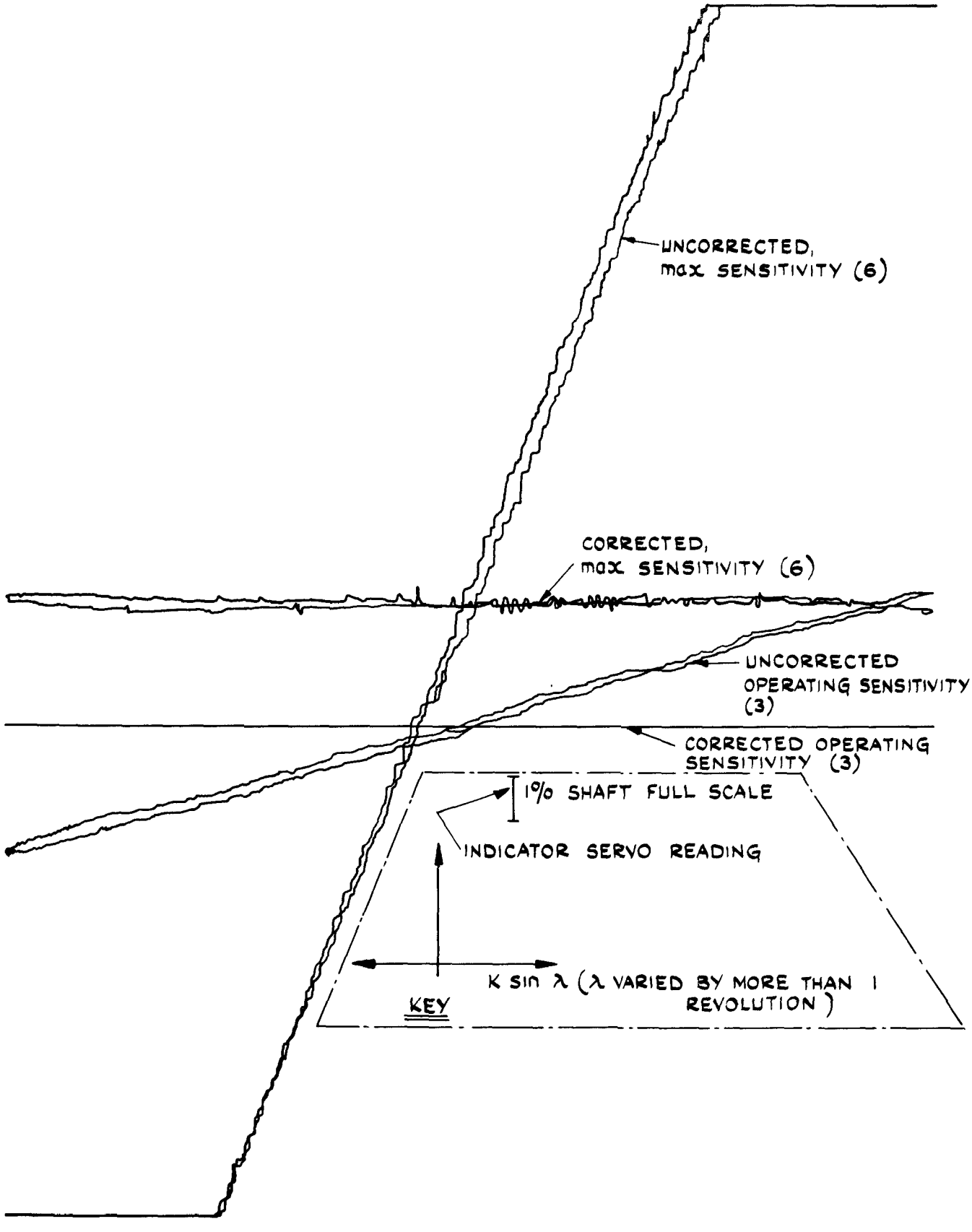

FIG. 3 TYPICAL TARE CORRECTION AT MAXIMUM AND OPERATING INDICATOR SENSITIVIES

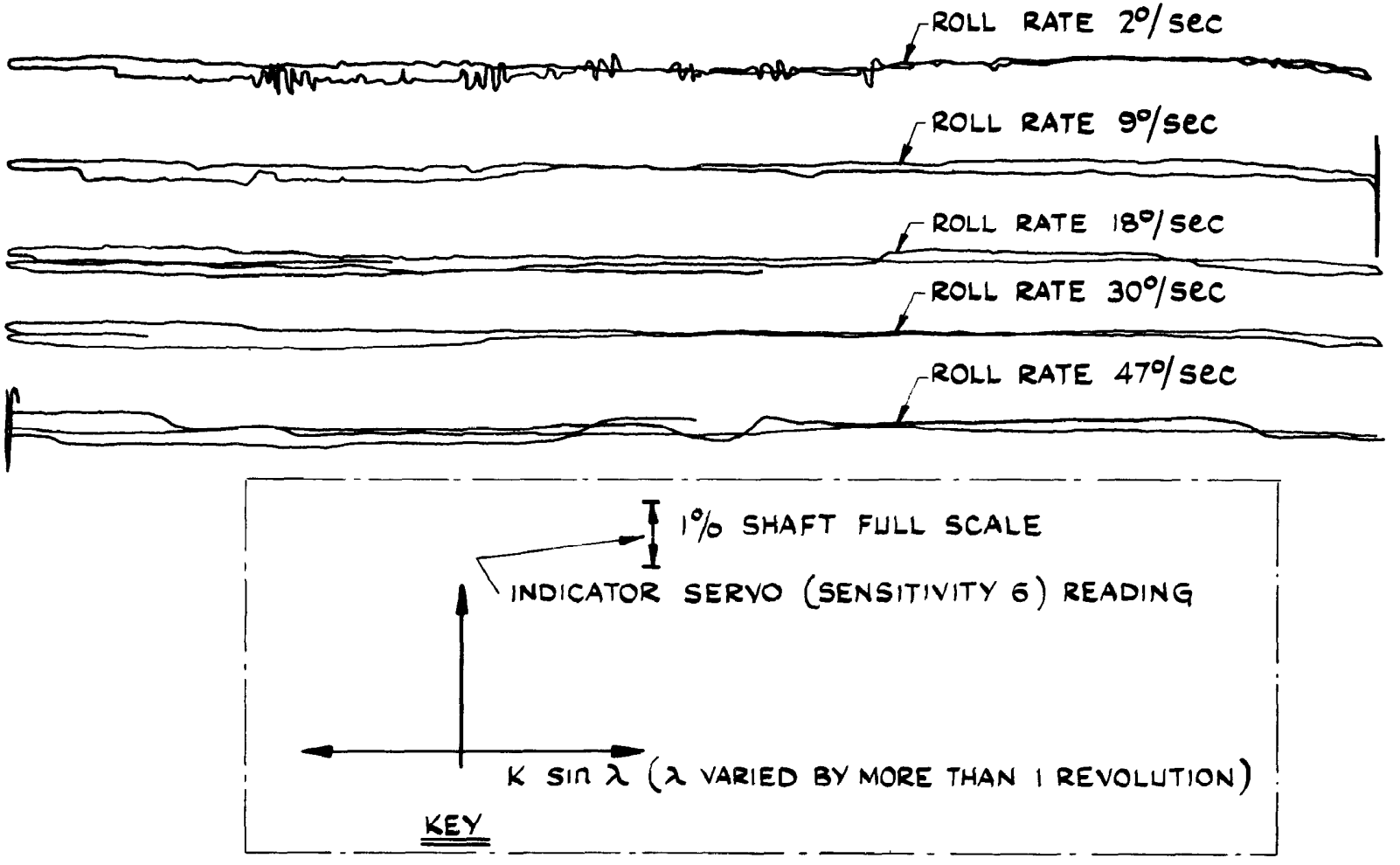

FIG. 4 EFFECT OF VARYING ROLL RATE ON TARE CORRECTION— MAXIMUM INDICATOR SENSITIVITY

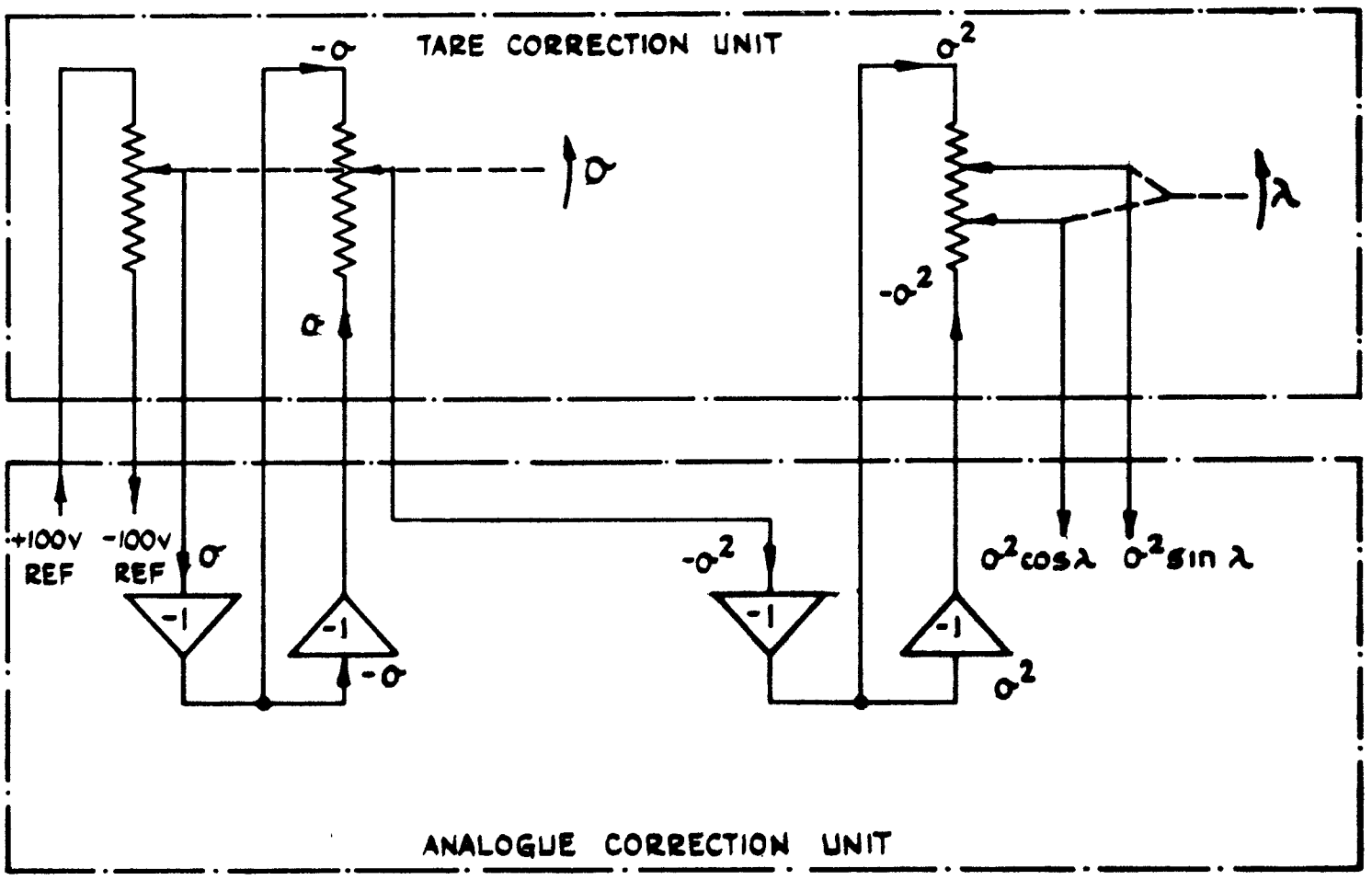

FIG. 5 GENERATION OF TARE CORRECTION TERMS $\sigma^2 \sin \lambda$ AND $\sigma^2 \cos \lambda$

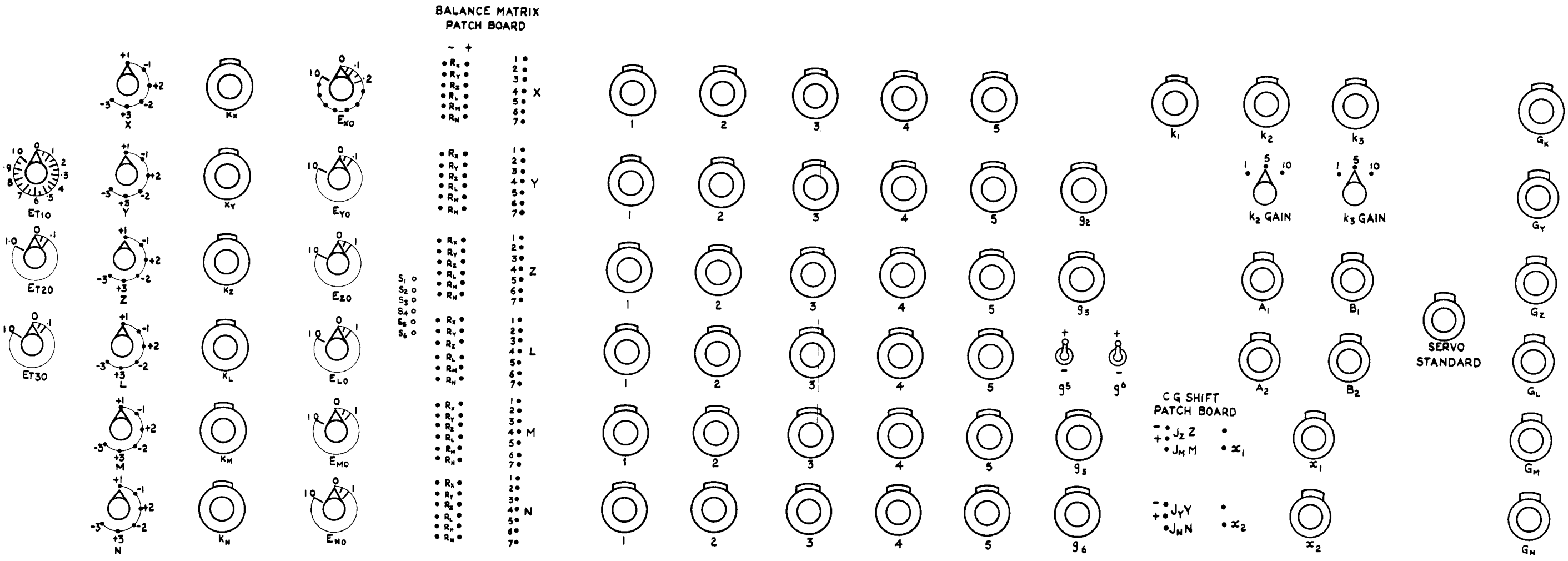

FIG. 6 LAYOUT OF PROGRAMME PANEL. ANALOGUE CORRECTION UNIT.

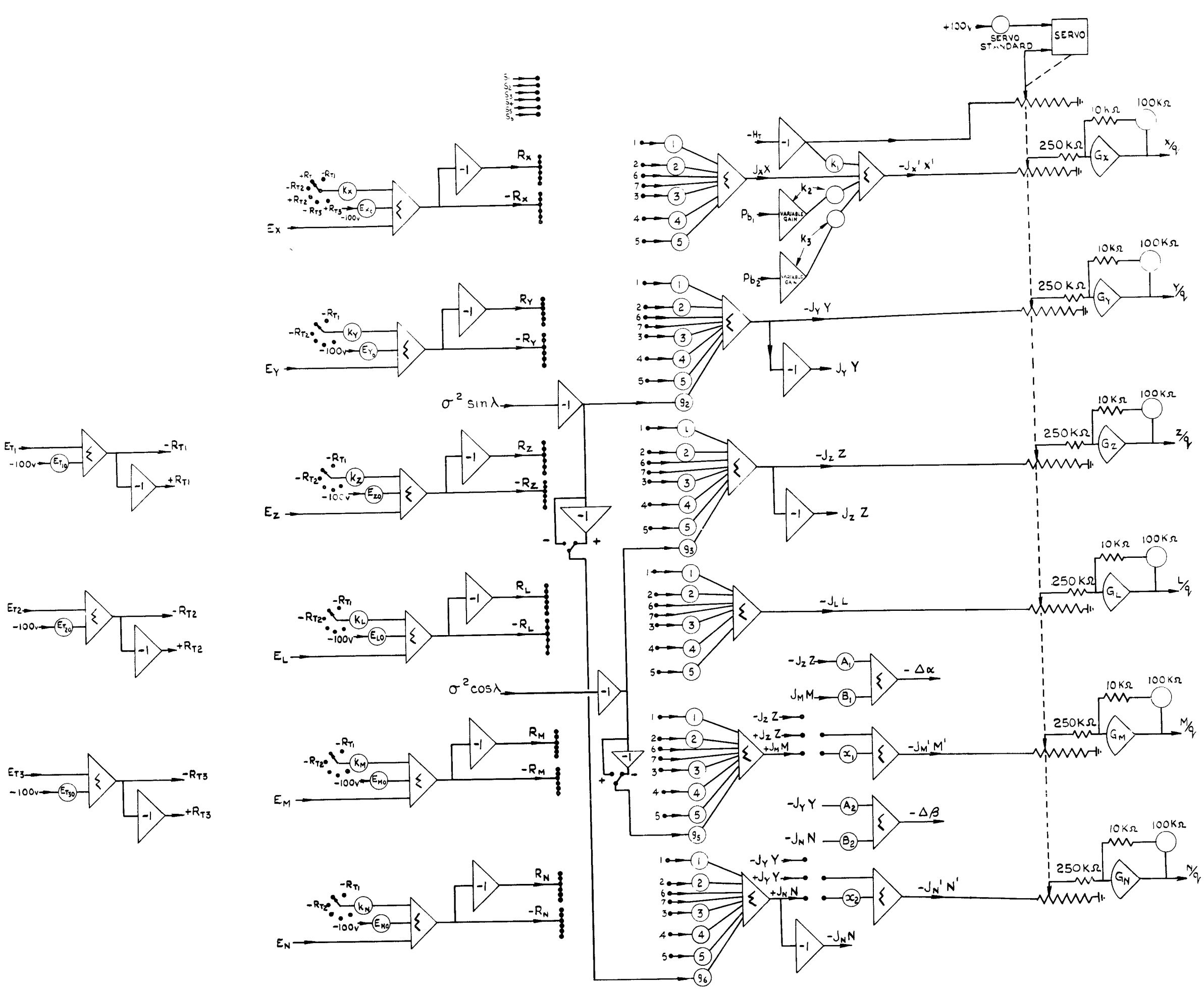

FIG.7 SCHEMATIC LAYOUT. ANALOGUE CORRECTION UNIT.

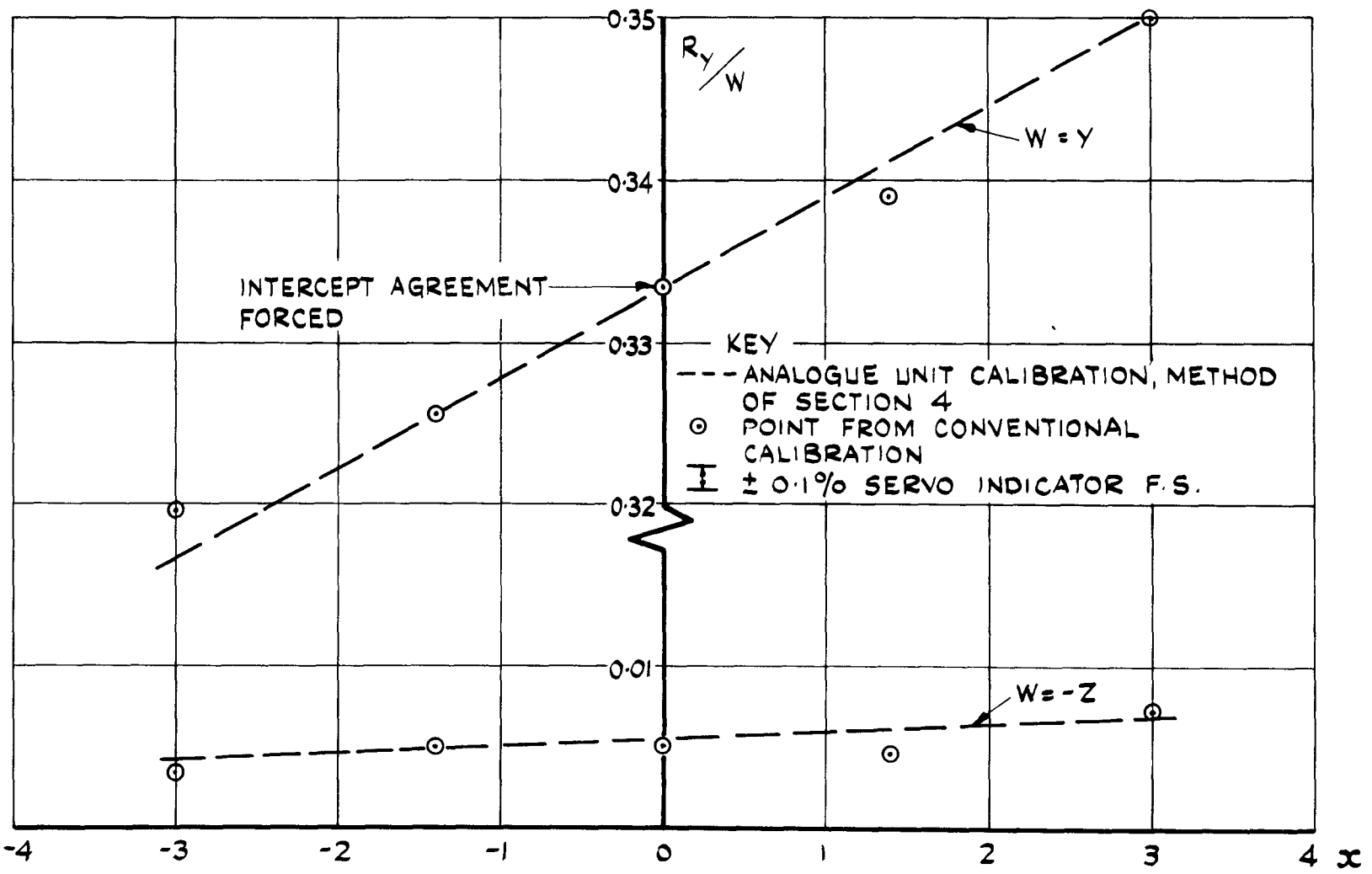

FIG. 8 COMPARISON OF CALIBRATION RESULTS, Y CHANNEL

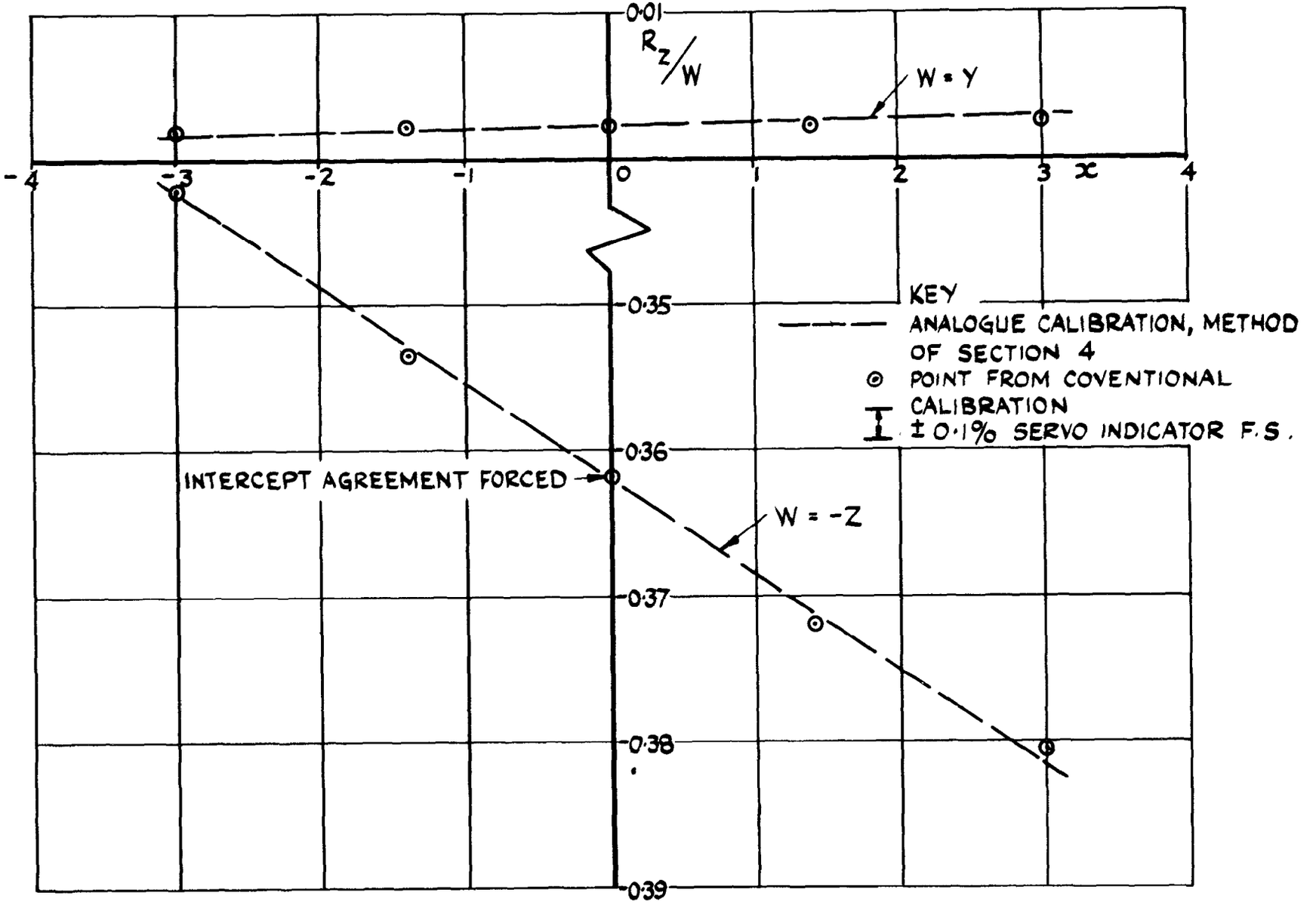

FIG. 9 COMPARISON OF CALIBRATION RESULTS, Z CHANNEL

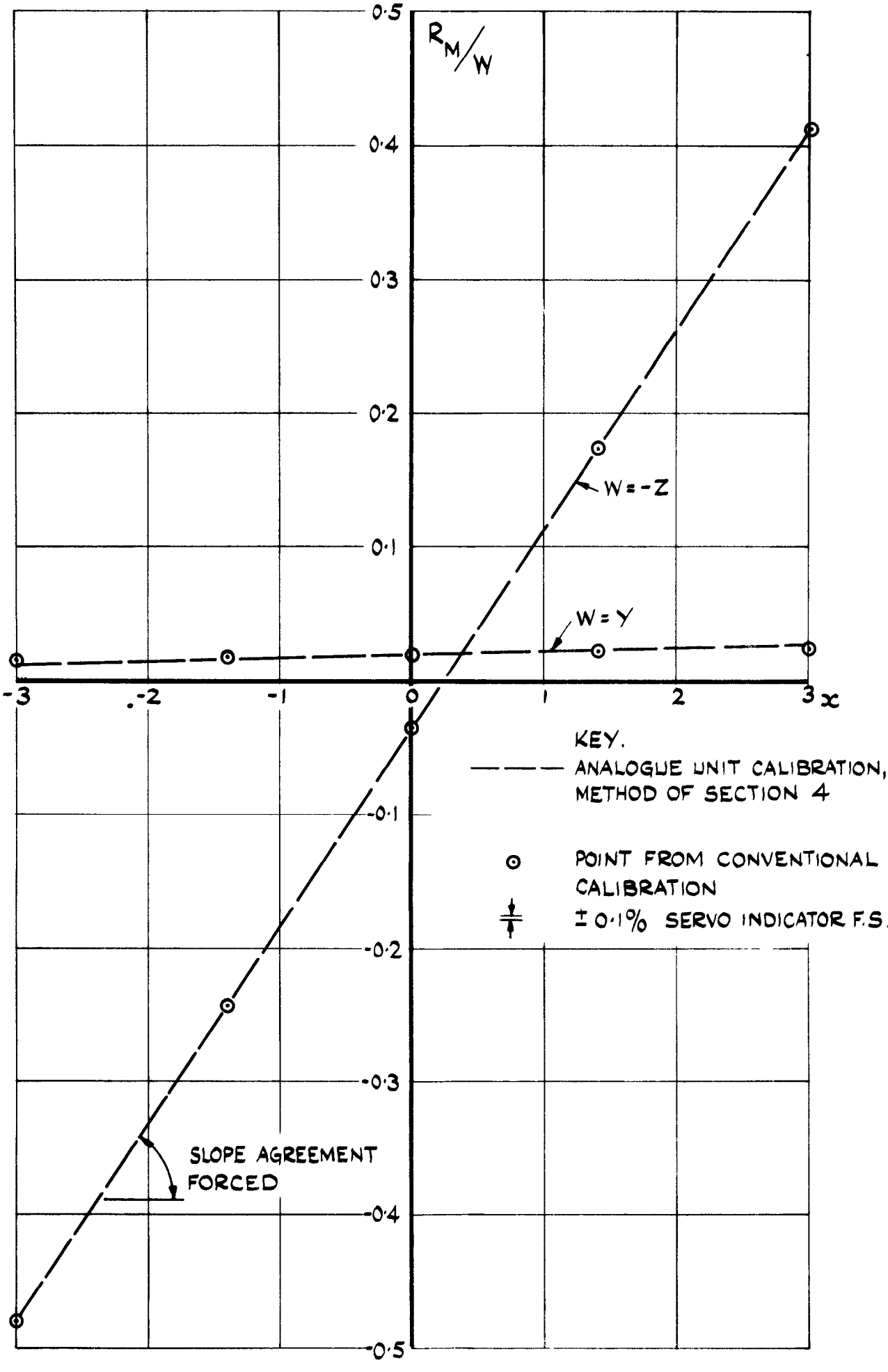

FIG. 10 COMPARISON OF CALIBRATION RESULTS, M CHANNEL

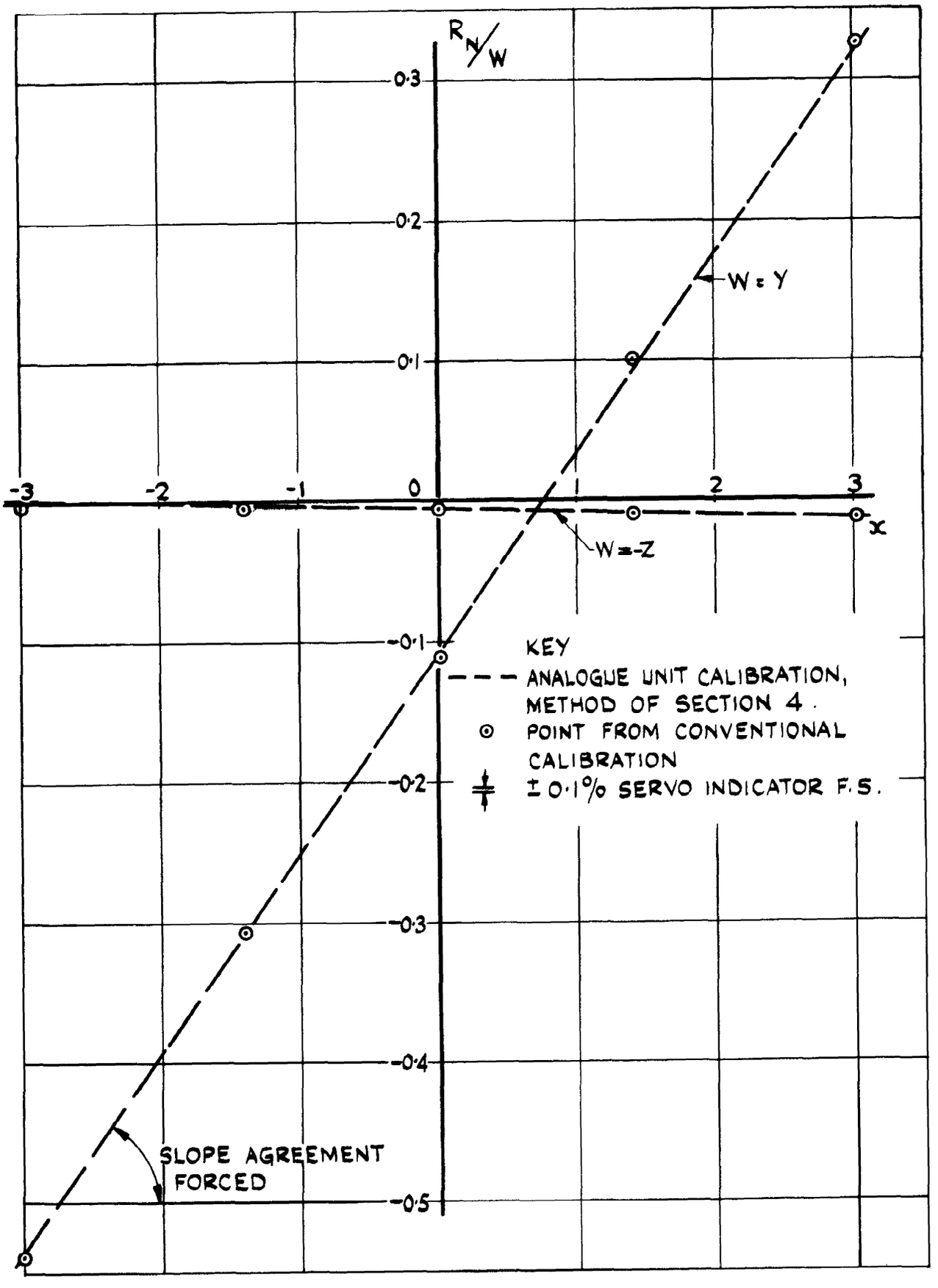

FIG. 11 COMPARISON OF CALIBRATION RESULTS, N CHANNEL

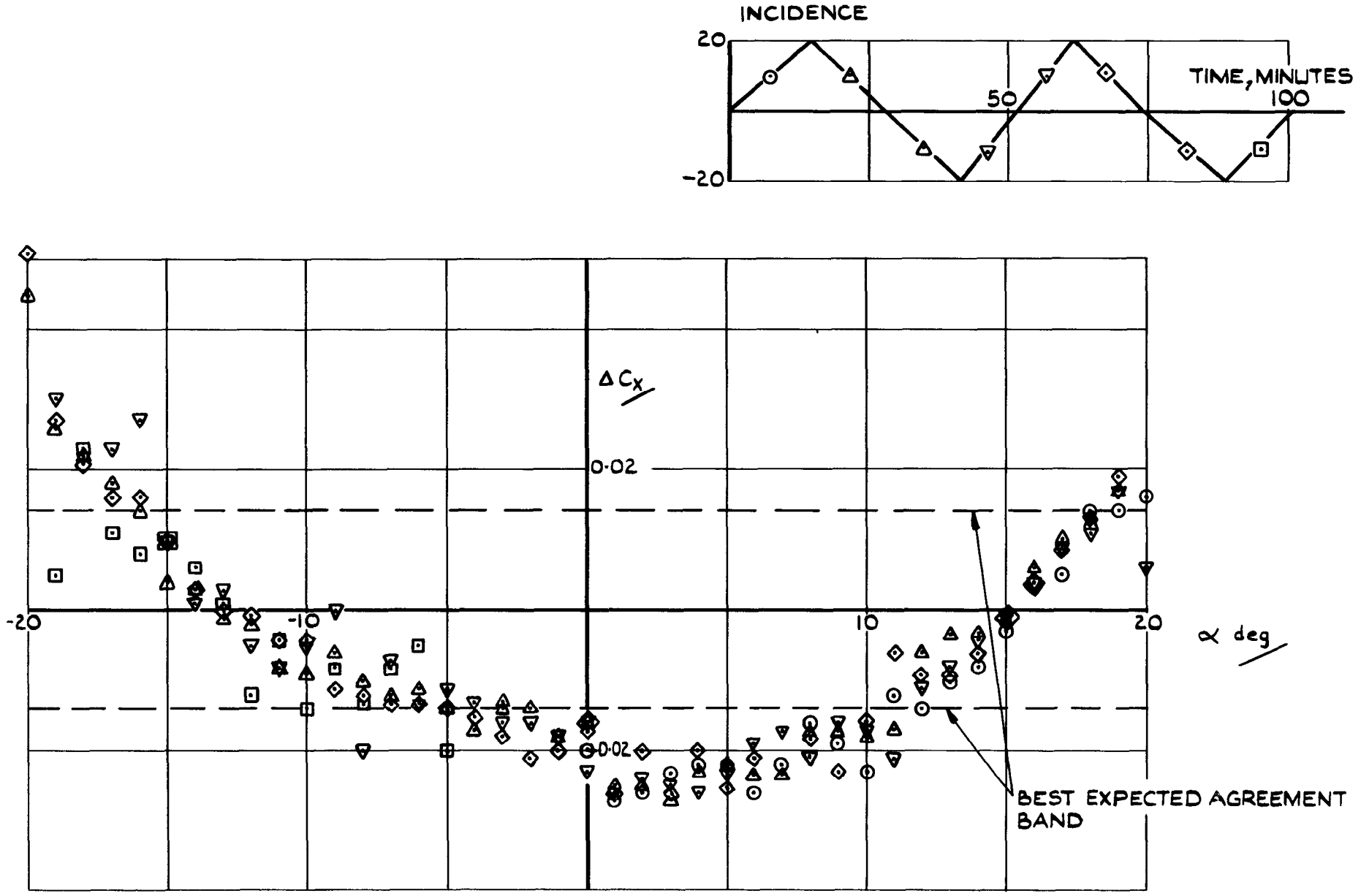

FIG.12 DISCREPANCIES IN C_X COMPUTATIONS

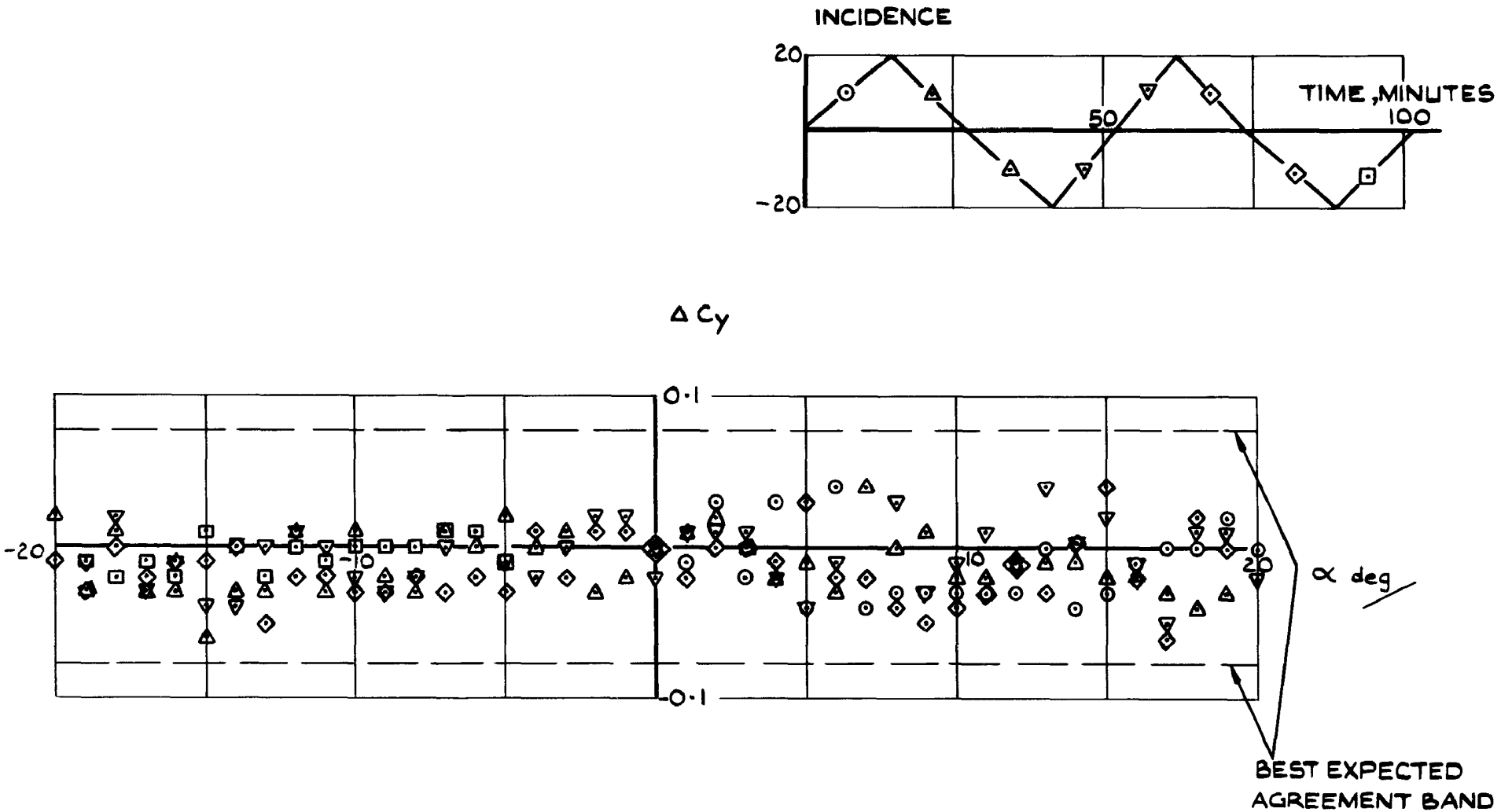

FIG.13 DISCREPANCIES IN C_y COMPUTATIONS

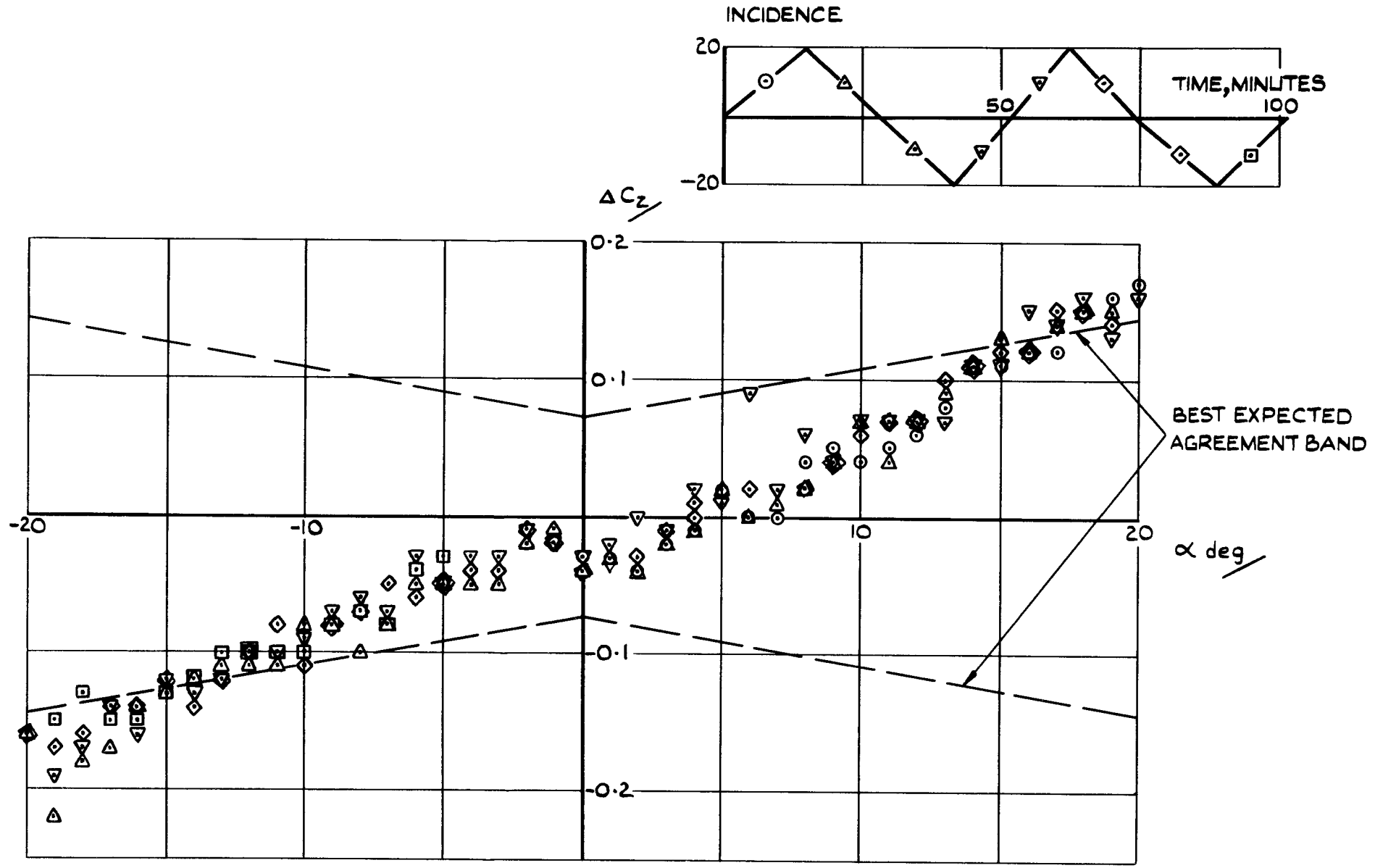

FIG. 14 DISCREPANCIES IN C_Z COMPUTATIONS

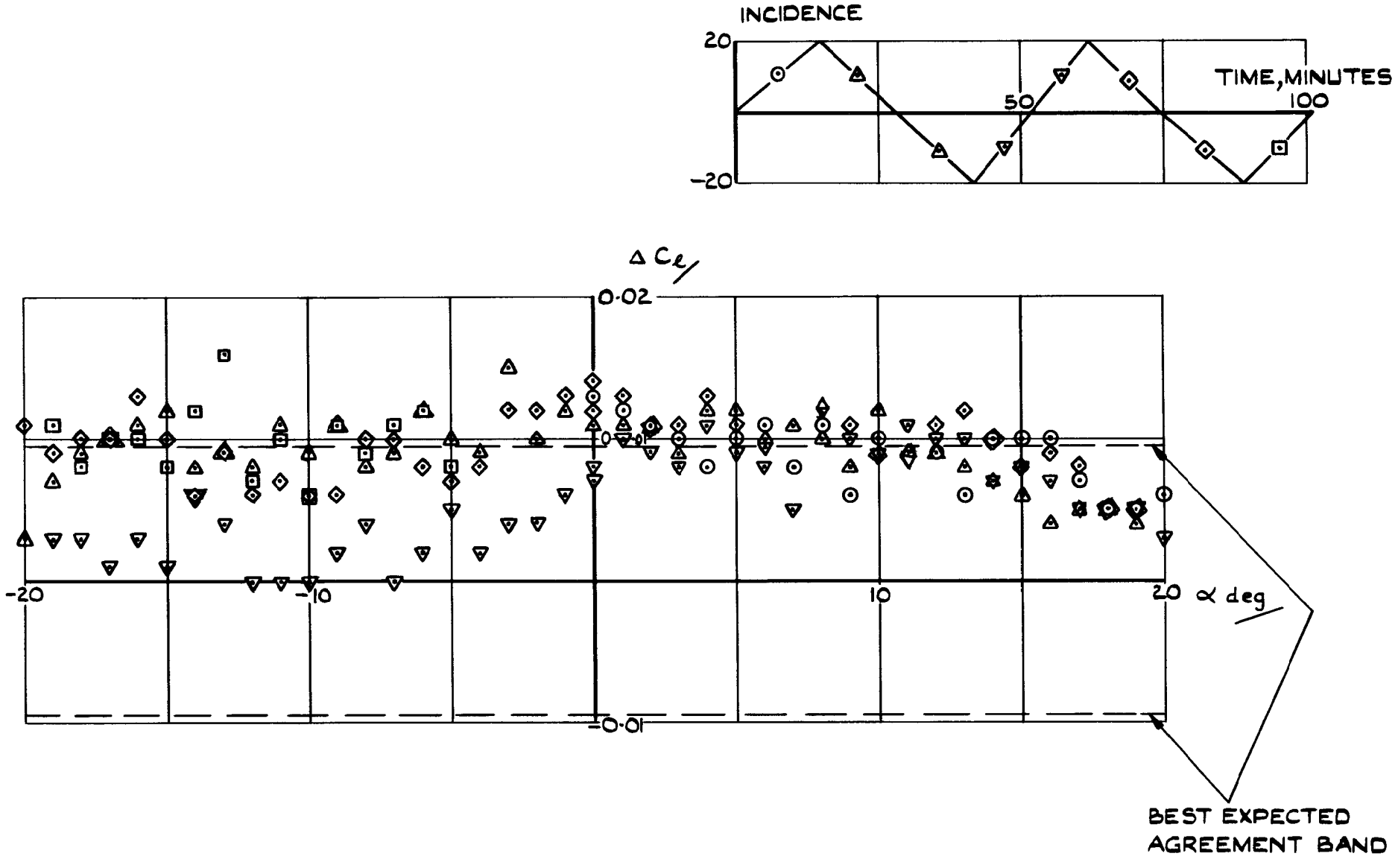

FIG. 15 DISCREPANCIES IN C_ℓ COMPUTATIONS

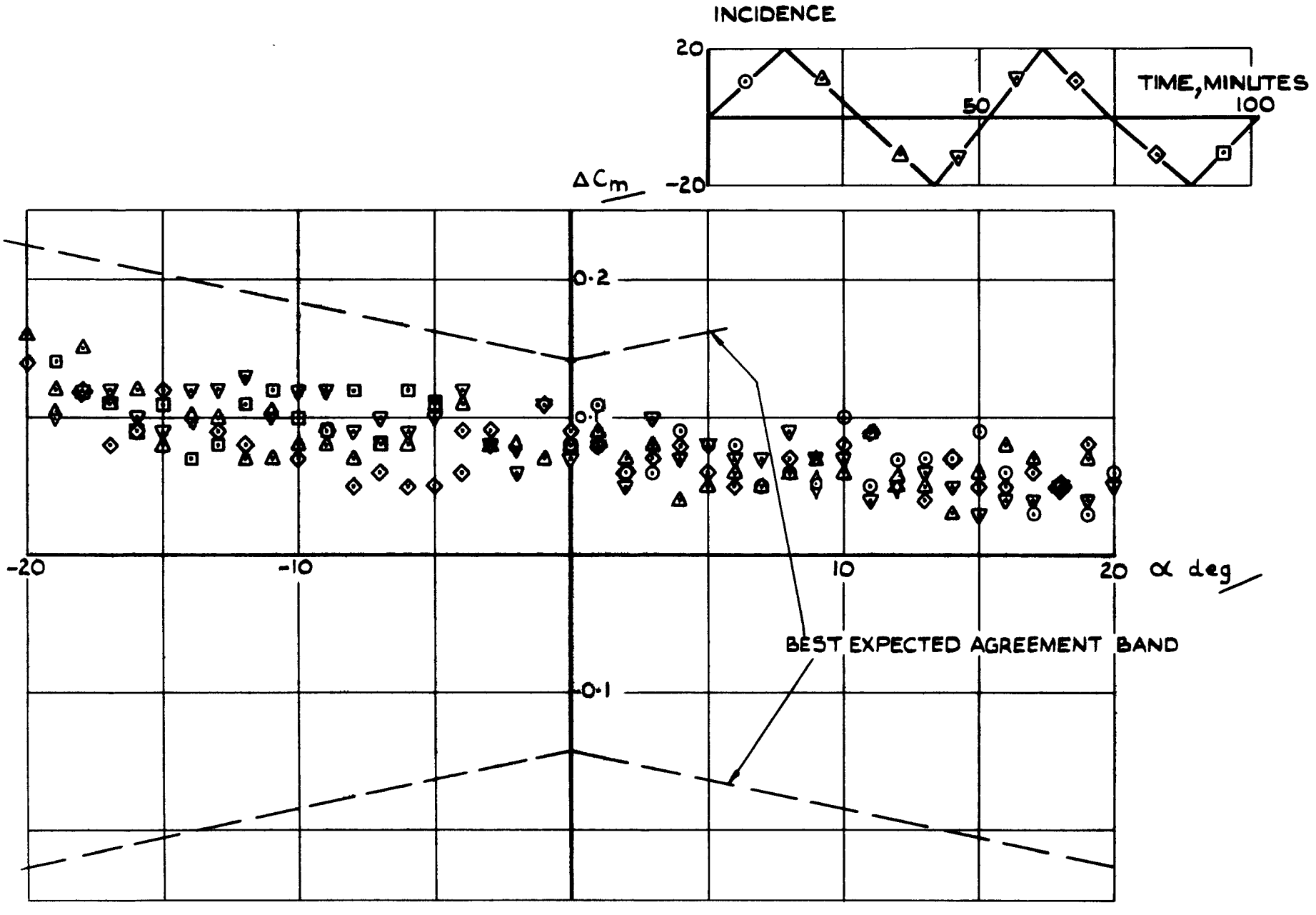

FIG.16 DISCREPANCIES IN C_m COMPUTATIONS

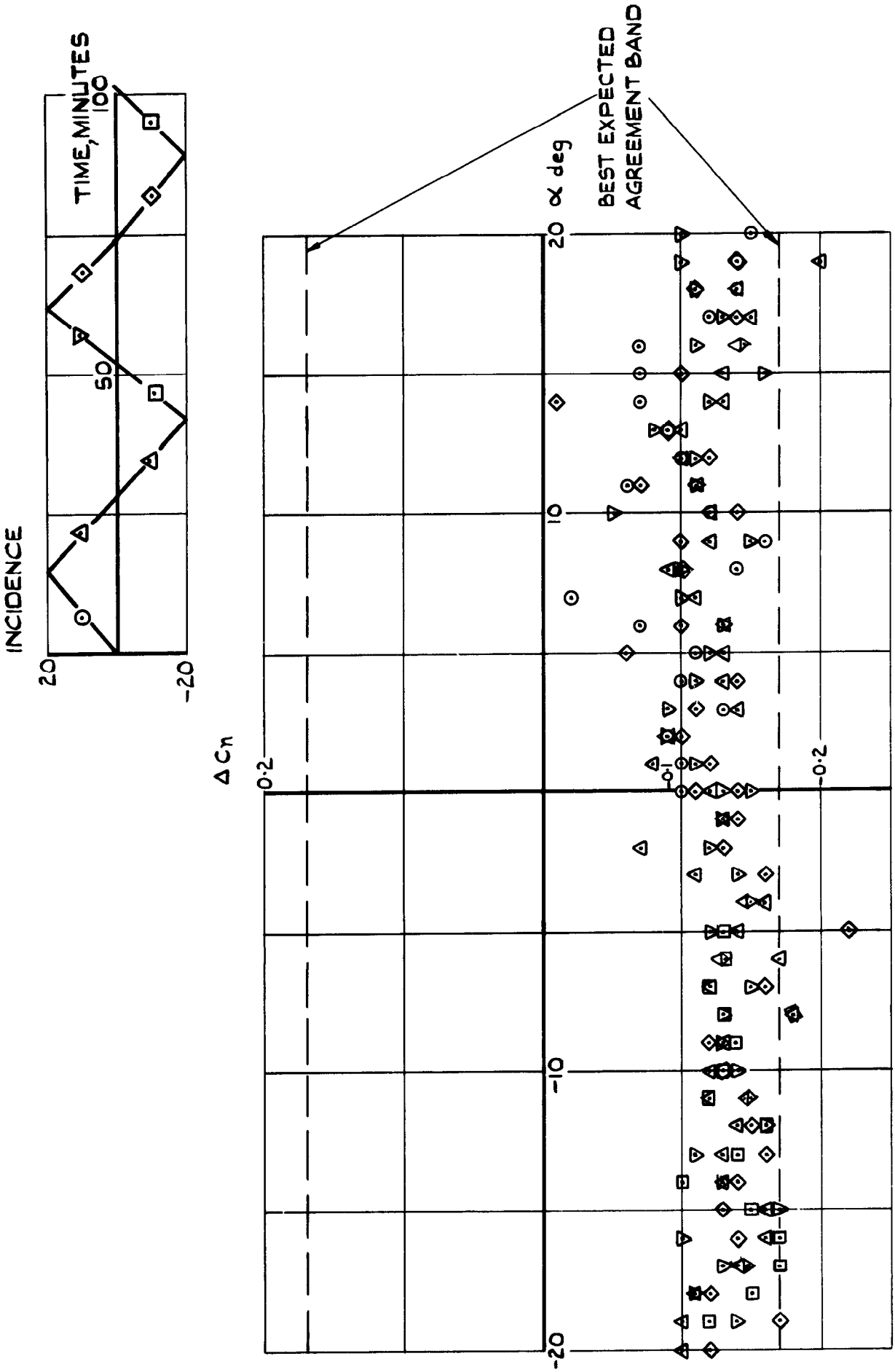

FIG. 17 DISCREPANCIES IN C_n COMPUTATIONS

Printed in England for Her Majesty's Stationery Office by the Royal Aircraft Establishment, Farnborough. Dd.125875.K4.

A.R.C. C.P. No.946
October 1966
Pecover, B.E.
AN ANALOGUE COMPUTER FOR ON-LINE CORRECTION OF WIND TUNNEL FORCE AND MOMENT DATA

681.14 :
621.317.79 :
533.6.071 :
533.6.011.5 :
533.6.013.11 :
533.6.013.15 :
531.71

A description is given of equipment using analogue computing techniques for the on-line correction of wind tunnel force and moment data, derived from strain-gauge indicator servos operating with a supersonic wind tunnel.

This equipment has enabled a new method of balance calibration to be employed which considerably reduces the possibilities of error and is quicker than previous methods.

(over)

A.R.C. C.P. No.946
October 1966
Pecover, B.E.
AN ANALOGUE COMPUTER FOR ON-LINE CORRECTION OF WIND TUNNEL FORCE AND MOMENT DATA

681.14 :
621.317.79 :
533.6.071 :
533.6.011.5 :
533.6.013.11 :
533.6.013.15 :
531.71

A description is given of equipment using analogue computing techniques for the on-line correction of wind tunnel force and moment data, derived from strain-gauge indicator servos operating with a supersonic wind tunnel.

This equipment has enabled a new method of balance calibration to be employed which considerably reduces the possibilities of error and is quicker than previous methods.

(over)

A.R.C. C.P. No.946
October 1966
Pecover, B.E.
AN ANALOGUE COMPUTER FOR ON-LINE CORRECTION OF WIND TUNNEL FORCE AND MOMENT DATA

681.14 :
621.317.79 :
533.6.071 :
533.6.011.5 :
533.6.013.11 :
533.6.013.15 :
531.71

A description is given of equipment using analogue computing techniques for the on-line correction of wind tunnel force and moment data, derived from strain-gauge indicator servos operating with a supersonic wind tunnel.

This equipment has enabled a new method of balance calibration to be employed which considerably reduces the possibilities of error and is quicker than previous methods.

(over)

DETACHABLE ABSTRACT CARDS

Accuracy is discussed and comparisons made between results obtained from the new equipment and those obtained by earlier, digital techniques.

Accuracy is discussed and comparisons made between results obtained from the new equipment and those obtained by earlier, digital techniques.

Accuracy is discussed and comparisons made between results obtained from the new equipment and those obtained by earlier, digital techniques.

Published by
HER MAJESTY'S STATIONERY OFFICE.

To be purchased from
49 High Holborn, London W.C.1
423 Oxford Street, London W.1
13A Castle Street, Edinburgh 2
109 St. Mary Street, Cardiff
Brazennose Street, Manchester 2
50 Fairfax Street, Bristol 1
35 Smallbrook, Ringway, Birmingham 5
7-11 Linenhall Street, Belfast 2
or through any bookseller

C.P. No. 946

S.O. CODE No. 23-9017-46